Chapter 1
Olefin Polymerization with Metallocene Catalysts

Takeshi Shiono

Abstract This chapter firstly explains the basic terms and concepts concerning olefin polymerization and polymer synthesis, and then provides comprehensive yet concise commentaries on olefin polymerization by metallocene catalysts. In Sect. 1.1 (Introduction), the history of olefin polymerization catalysts is briefly reviewed with a focus on the uniformity of the active species. In Sect. 1.2 are described the elementary process of olefin polymerization by transition metal catalysts and the molecular weight distributions of produced polymers. The tacticity and stereoregularity of vinyl polymer are explained in Sect. 1.3, where the relation between the microtacticity of the stereoregular polymer and the mechanism of stereospecific polymerization is described in detail. Section 1.4 deals with copolymerization with two kinds of monomers on the basis of kinetics and probability theory. In Sect. 1.5, are described the basics of metallocene catalysts and their characteristics in propylene polymerization and copolymerization of olefins.

1.1 Introduction

Polyolefins are currently the most important synthetic polymers with the largest commercial production. Polyethylene and polypropylene are representative polyolefins. Polyethylene is classified into three categories, i.e., low-density polyethylene produced by high-pressure radical polymerization, high-density polyethylene and linear low-density polyethylene, which are homo- and copolymers of ethylene with 1-alkene, obtained by Phillips and Ziegler–Natta catalysts. Polypropylene possessing stereoregular structure is produced only by Ziegler–Natta catalysts. Since the great finding of Ziegler [1] and Natta [2], many

T. Shiono (✉)
Graduate School of Engineering (A4-822), Hiroshima University, Hiroshima, Japan
e-mail: tshiono@hiroshima-u.ac.jp

K. Osakada (ed.), *Organometallic Reactions and Polymerization*,
Lecture Notes in Chemistry 85, DOI: 10.1007/978-3-662-43539-7_1,

researchers have paid enormous effort to improve the catalytic performance of heterogeneous Ti-based Ziegler–Natta catalysts such as activity, the control of molecular weight and molecular weight distribution, copolymerization ability, stereospecificity, the control of polymer particle size and shape, etc. Consequently, highly active $MgCl_2$-supported $TiCl_4$ catalysts are widely used for the commercial production of polyethylene and polypropylene [3, 4].

Homogeneous Ziegler–Natta catalysts composed of titanocene compound and alkylaluminum were also found in the middle of 1950s [5, 6]. Their application had been limited to the basic study because they showed low activity in ethylene polymerization and no activity in propylene polymerization. However, it was reported that the addition of a small amount of water improved the catalytic activity of those systems [7]. Sinn and Kaminsky isolated the condensation product of trimethylaluminum and water, i.e., methylaluminoxane (MAO), and applied it as a cocatalyst for zirconocene and titanocene compounds to obtain highly active homogeneous Ziegler–Natta catalysts for ethylene and propylene polymerizations [8]. The catalytic system was found to be active also for homo- and copolymerization of higher 1-alkene or cycloolefin with ethylene as well as for stereospecific polymerization of propylene by tuning the metallocene used [9]. The activation methods except MAO were developed and the homogeneous systems were successfully heterogenized in order to apply them to slurry phase or gas phase process [10, 11]. These catalytic systems which composed of a metallocene compound are called metallocene catalysts.

Most important characteristics of metallocene catalysts is the uniformity of the active species regardless of the phase of the catalytic systems, which gives uniform polymers with respect to molecular weight distribution, comonomer composition, stereoregularity, etc. Those uniform polyolefins cannot be obtained with $TiCl_3$- or $TiCl_4$-based heterogeneous Ziegler–Natta catalysts because of their non-uniformity of the active species. The words “homogeneous” and “heterogeneous” are usually used to describe the phase of catalytic systems, but a homogeneous catalyst does not necessarily gives homogeneous (uniform) active species. In order to clarify the homogeneity or the inhomogeneity of active species in a polymerization catalyst, we currently use the word “single-site” or “multi-site”.

The founding of metallocene catalysts stimulated the research on the polymerization catalysts composed of well-characterized transition metal complexes, which has evolved in a variety of single-site catalysts such as half metallocene catalysts (composed of a monocyclopentadienyl compound), constrained geometry catalyst (composed of an *ansa*-(cyclopentadienyl)(amido) compound), Brookhart catalyst (composed of a late transition metal diimine compound), FI catalyst (composed of a bis(phenoxyimine) compound) [12].

This chapter first explains the basic terms and the concepts in the fields of polymer chemistry and olefin polymerization catalysis, and then describes the characteristics of metallocene catalysts.

1.2 Elementary Processes of Olefin Polymerization

1.2.1 Initiation and Propagation Reactions

Olefin polymerization with Ziegler–Natta catalyst is initiated by the coordination of olefin to a coordinatively unsaturated transition metal–alkyl or metal–hydride species followed by the insertion of the coordinated olefin (Eq. 1.1).

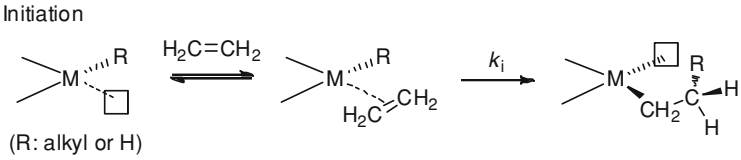

(1.1)

Olefin coordination to a transition metal is dominated by the σ-bond via the electron donation of the C=C π bond to the empty *d* orbital on the metal and the back donation from the filled metal *d* orbital to the empty π* orbital as shown Fig. 1.1.

The insertion reaction proceeds via alkyl migration to the coordinated olefin (*cis*-addition), and successive multiple coordination-insertions of olefins propagate a polymer chain. This type of polymerization is therefore classified to coordination polymerization. If steady-state approximation is applied to the olefin-coordinated metal–alkyl species, propagation rate R_p is expressed by Eq. 1.3, where [C*] and [M] are the concentrations of active species and monomer, respectively. When the coordination of monomer is very strong or very weak, Eq. 1.3 can be approximated by $R_p = k_p$ [C*] or $R_p = \{k_p k_M/(k_{-M} + k_p)\}$ [C*] [M], respectively.

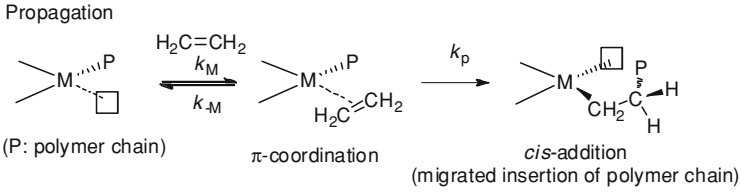

(1.2)

$$R_p = \frac{k_p\, k_M\, [C^*]\, [M]}{k_M\, [M] + k_{-M} + k_p} \qquad (1.3)$$

R_p: polymerization rate
[C*]: number of active species
[M]: monomer concentration

1.2.2 Chain Transfer and Termination Reaction

Main chain transfer reactions in olefin polymerization with Ziegler–Natta catalyst is β-hydrogen transfer to the coordinated olefin (Eq. 1.4) or to the metal center

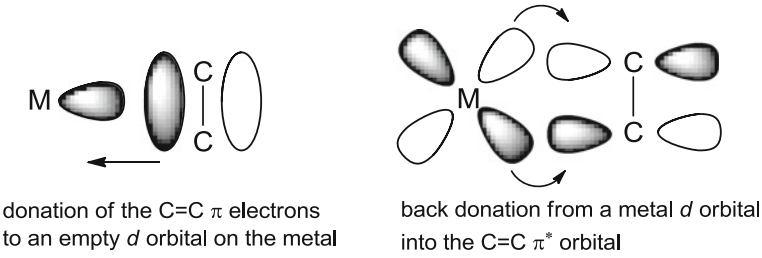

Fig. 1.1 Coordination mode of olefin to a transition metal

(Eq. 1.5), and the alkyl exchange between the active species and an alkylmetal used as a cocatalyst (Eq. 1.6).

Chain transfer

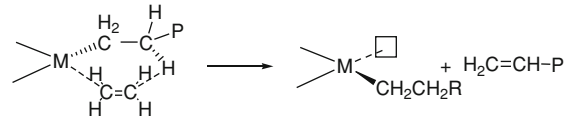

(1.4)

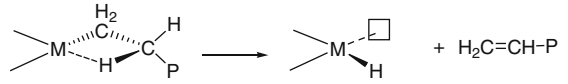

(1.5)

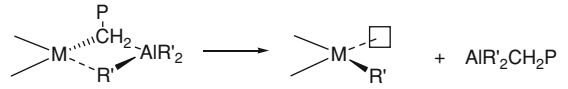

(1.6)

In a commercial process, hydrogen gas is used as a chain transfer reagent (Eq. 1.7).

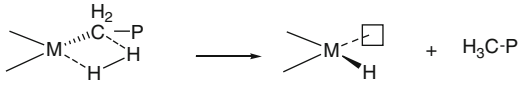

(1.7)

In all cases, transition metal–alkyl or metal–hydride is regenerated and the propagation reaction continues.

Termination reaction, i.e., the deactivation of catalyst is considered to proceed via homolytic cleavage of the transition metal–polymer bond by unimolecular or bimolecular process to cause the reduction of the active transition metal.

1.2.3 Molecular Weight and Molecular Weight Distribution

1.2.3.1 Average Molecular Weight

Every synthetic polymer contains molecules of various degrees of polymerization or molecular weight. This state of affairs is described that the polymer shows polydispersity with respect to degree of polymerization or molecular weight. Accordingly, we can obtain the degree of polymerization or the molecular weight of polymer only as an average value. The number-average polymerization degree $\bar{P}_n$ and the weight-average polymerization degree $\bar{P}_w$ are defined by Eqs. 1.8 and 1.9 where x is a polymerization degree of a certain polymer chain "x-mer" and N_x is the number of x-mer. The number-average and the weight-average molecular weights, $\overline{M}_n$ and $\overline{M}_w$, are obtained by multiplying the molecular weight of the monomer, M_0, to $\bar{P}_n$ and $\bar{P}_w$, respectively (Eqs. 1.10 and 1.11).

$$\bar{P}_n = \frac{\sum x \cdot N_x}{\sum N_x} \tag{1.8}$$

$$\bar{P}_w = \frac{\sum x^2 \cdot N_x}{\sum x \cdot N_x} \tag{1.9}$$

$$\overline{M}_n = \overline{P}_n M_0 \tag{1.10}$$

$$\overline{M}_w = \overline{P}_w M_0 \tag{1.11}$$

1.2.3.2 Molecular Weight Distribution

In vinyl-addition polymerization, the molecular weight of the produced polymer is determined by the relative ratio of propagation and termination reactions. Suppose that coordination polymerization proceeds in a steady state, and put the propagation rate and the total rate of chain transfer and termination as r_p and Σr_{tr}, respectively. Then, the propagation probability α is given by

$$\alpha = \frac{r_p}{r_p + \sum r_{tr}} \tag{1.12}$$

The mole fraction of "x-mer", $f_n(x)$, is shown by Eq. 1.13, because "x-mer" forms via $(x - 1)$ times of propagation followed by termination.

$$f_n(x) = \alpha^{x-1} \cdot (1 - \alpha) \tag{1.13}$$

The weight fraction of "x-mer", $f_w(x)$, is

$$f_w(x) = x \cdot \alpha^{x-1} \cdot (1-\alpha)^2 \tag{1.14}$$

Please note $f_n(x)$ and $f_w(x)$ are normalized. Referring Eqs. 1.8 and 1.9, $\overline{P}_n$ and $\overline{P}_w$ are expressed by $f_n(x)$ and x, and converted to the equations with α by summation of series with x.

$$\overline{P}_n = \sum_{x=1}^{\infty} x \cdot f_n(x) = \frac{1}{1-\alpha} \tag{1.15}$$

$$\overline{P}_w = \sum_{x=1}^{\infty} x \cdot f_w(x) = \frac{1+\alpha}{1-\alpha} \tag{1.16}$$

Thus, we obtain $\overline{P}_w/\overline{P}_n$ ($\overline{M}_w/\overline{M}_n$) as

$$\overline{P}_w/\overline{P}_n = \overline{M}_w/\overline{M}_n = 1+\alpha \tag{1.17}$$

This ratio is named the polydispersity index (PDI) or the polydispersity. When high molecular-weight polymer is obtained, α should be close to one. Thus $\overline{M}_w/\overline{M}_n = 2$. Figure 1.2 illustrates the distribution of x-mer in the polymers with $\overline{P}_n = 10$ ($\alpha = 0.9$) and $\overline{P}_n = 100$ ($\alpha = 0.99$).

If the system is not uniform chemically or physically with respect to the propagation probability α, PDI becomes more than 2.

It should be noted that Eqs. 1.13–1.17 are the same with those of condensation polymerization by substituting α with p; p is an extent of polymerization. α is independent of polymerization time in a steady state, whereas p reaches to unity with the progress of polymerization. Although α and p have a different definition, both parameters imply the bonding probability of the neighboring monomers. The molecular weight distribution expressed by Eqs. 1.13 or 1.14 are called the most probable (or Schulz–Flory) distribution.

1.2.3.3 Living Polymerization

In an ideal living polymerization, all the active species simultaneously initiate the polymerization, with the rate constant for initiation greater than that for propagation and with neither chain transfer nor termination. Under these conditions, we can obtain a polymer with very narrow molecular weight distribution. The kinetic treatment on this model, where polymerization time is replaced with a number of average polymerized monomer per one active species v, gives $f_n(x)$ and $f_w(x)$ as Poisson distribution.

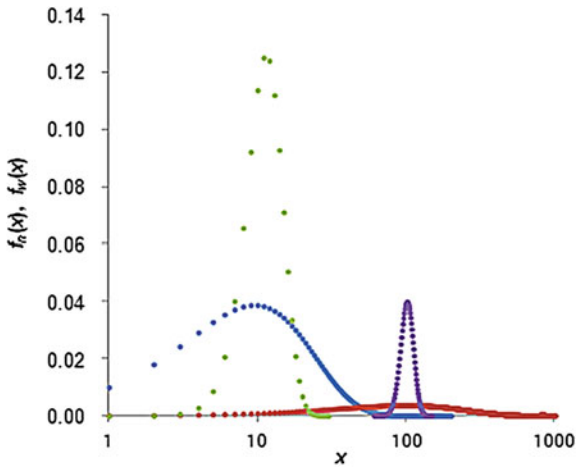

Fig. 1.2 Distribution of x-mer in the polymers with $\overline{P}_n = 10$ and $\overline{P}_n = 100$: ●, ●, the most probable distribution; ●, ●, Poisson distribution

$$f_n(x) = \frac{v^{x-1}}{(x-1)!} \cdot e^{-v} \tag{1.18}$$

$$f_w(x) = \frac{v}{v+1} \cdot x \cdot \frac{v^{x-2}}{(x-1)!} \cdot e^{-v} \tag{1.19}$$

$\overline{P}_n$ and $\overline{P}_w$ expressed by x and $f_n(x)$ are converted to the function of v by summation of series with x,

$$\overline{P}_n = v + 1 \tag{1.20}$$

$$\overline{P}_w = \frac{v^2 + 3v + 1}{v + 1} \tag{1.21}$$

The polydispersity index is

$$\frac{\overline{P}_w}{\overline{P}_n} = \frac{v^2 + 3v + 1}{(v+1)^2} = 1 + \frac{v}{(v+1)^2} \approx 1 + \frac{1}{v+1} = 1 + \frac{1}{\overline{P}_n} \tag{1.22}$$

where the approximation applies for large v. Equation 1.22 indicates that the polydispersity gets close to one according to the progress of polymerization. The distributions of x-mer in the polymers with $\overline{P}_n = 10$ ($v = 9$) and $\overline{P}_n = 100$ ($v = 99$) are illustrated in Fig. 1.2.

1.3 Structure of Vinyl Polymer and Stereospecific Polymerization

1.3.1 Stereoregularity of Vinyl Polymer

In the polymerization of substituted olefins such as propylene and methyl methacrylate, chiral carbons are induced in the main chain. If the molecular weight of the produced polymer is high enough to neglect the chain end structure of the initiation and the termination, we can only distinguish the relative configuration of the adjacent monomer units. In the adjacent two monomer units (diad), the substituted carbons have the same configuration or the opposite one. The former is meso denoted by m, and the latter is racemo denoted by r, respectively (Fig. 1.3). Then, the stereo structure, i.e., the tacticity of the adjacent three monomer units are expressed by mm (isotactic triad), rr (syndiotactic triad), and mr (or rm, heterotactic triad); mr and rm are identical in vinyl polymers.

An arbitrary stereo sequence can be expressed by the sequence of m and r. The polymer composed of m sequences, •••mmmmmm•••, that composed of r sequences, •••rrrrrr•••, and that composed of random sequences of m and r are named isotactic, syndiotactic and atactic, respectively [13]. The physical properties of vinyl polymers strongly depend on the stereoregularity of the polymers. The control of tacticity is therefore very important in vinyl polymerization.

The tacticity of vinyl polymer can be evaluated by NMR in principal. In the $^{13}C\{^{1}H\}$ NMR spectrum of polypropylene, the resonance of methylene carbon is split by diad tacticities and those of methyl and methine carbons are split by triad tacticities. These resonances are further split by the stereoregularity of the neighboring propylene units at both sides, i.e., tetrad and pentad tacticities, respectively. The resonance of methyl carbon is the most sensitive to the stereoregularity of polypropylene, and the pentad tacticities can be determined by 125 MHz $^{13}C\{^{1}H\}$ NMR (Fig. 1.4).

1.3.2 Regiochemistry in Propylene Polymerization

Coordination polymerization of olefin proceeds via insertion of coordinating monomer to metal–polymer bond. In the case of 1-alkene such as propylene, two insertion modes which differ in regiochemistry are possible; C1 carbon of olefin is attached to the metal (primary insertion or 1,2-insertion) or vice versa (secondary insertion or 2,1-insertion) (Fig. 1.5).

For the connection of the neighboring monomer units, there are three possibilities; C1 carbon connects to C2 carbon (head-to-tail), C1 carbon connects to C1 carbon (tail-to-tail), or C2 carbon connects to C2 carbon (head-to-head). The polymerization should proceed regioselectively in order to produce stereoregular polymers. The propylene polymerization with Ti-based heterogeneous

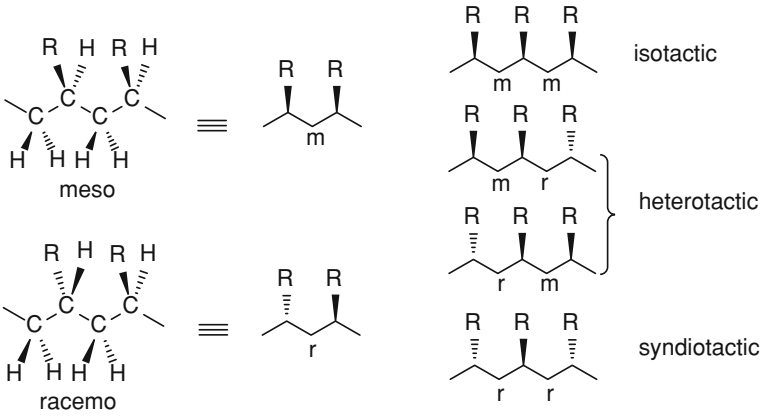

Fig. 1.3 Stereoregularity of vinyl polymer

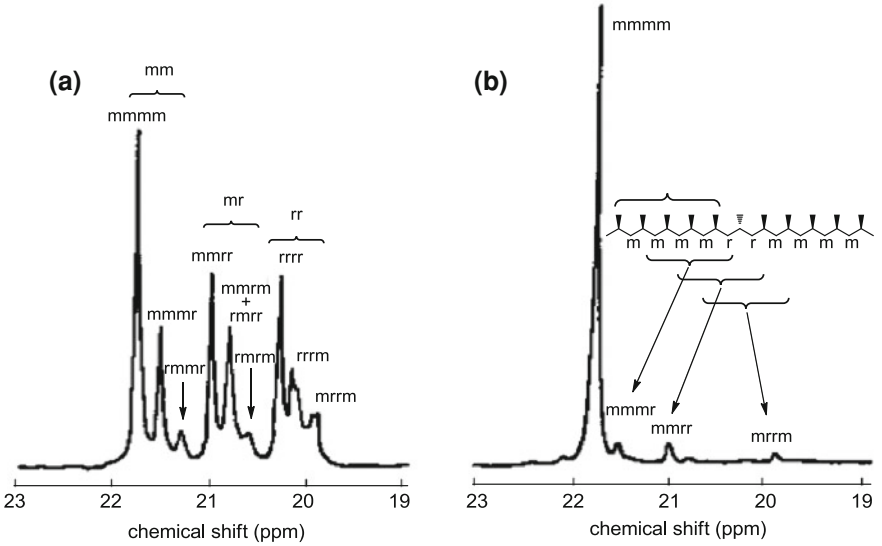

Fig. 1.4 125 MHz $^{13}C\{^{1}H\}$ NMR spectra of typical polypropylene obtained $TiCl_4/MgCl_2$–Et_3Al; **a** boiling heptane-soluble fraction, **b** boiling heptane-insoluble fraction

Ziegler–Natta catalysts and zirconocene catalysts proceeds via 1,2-insertion in high regioselectivity. Some zirconocene catalysts occasionally cause 2,1-insertion to give an isolated inverted unit or a tetramethylene unit via β-hydrogen elimination of methyl group and re-insertion (Fig. 1.6) [14, 15].

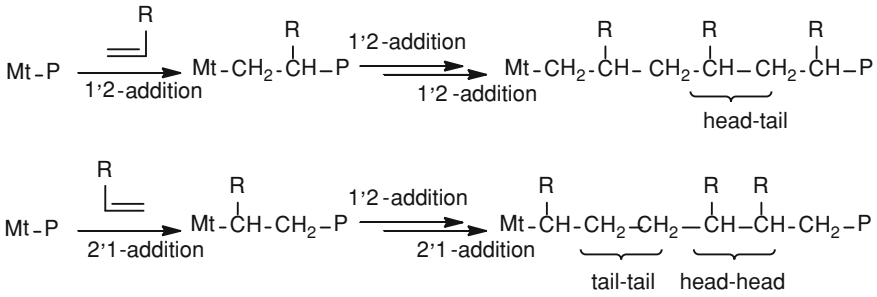

Fig. 1.5 Regiochemistry of propylene insertion to metal–polymer bond

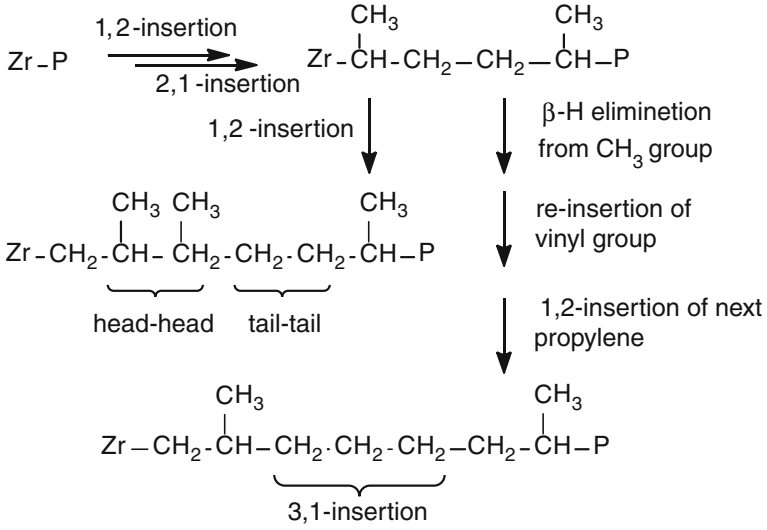

Fig. 1.6 3,1-insertion of propylene to Zr-polymer bond

1.3.3 Origin of Stereospecificity

Propylene is a prochiral molecule where sp^2-hybridized C2 carbon is converted to a chiral carbon when a metal–polymer bond is added to the *re* or *si* face of the molecule. Since the propagation proceeds via the coordination of propylene followed by the *cis*-addition of metal–polymer bond, the configuration of the chiral carbon induced in the main chain is determined when propylene coordinates to the metal center. Thus, the active species should differentiate the prochiral faces of propylene to achieve stereospecific polymerization.

In principal, the active species of propylene polymerization possess two chiral structures; one is the chiral carbon of the last-inserted propylene unit and the other

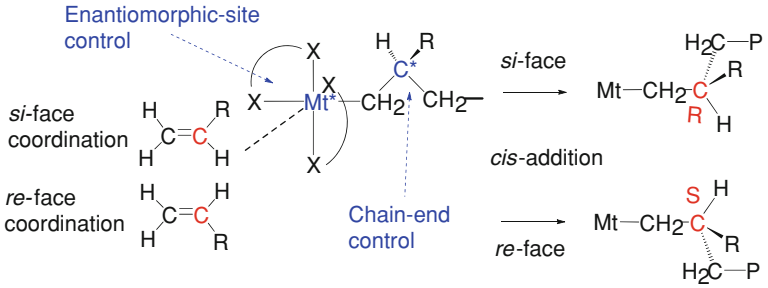

Fig. 1.7 Mechanism of stereospecific polymerization of 1-alkene

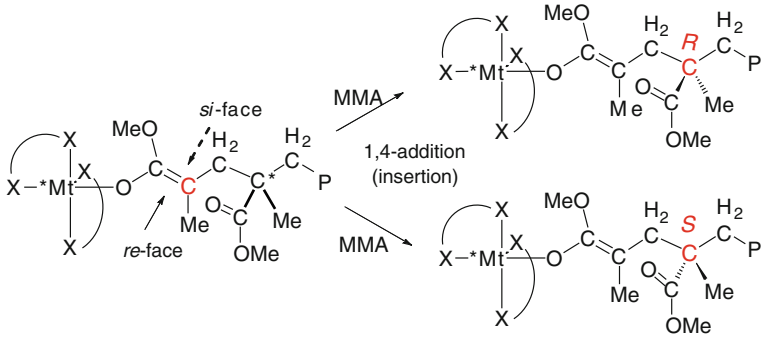

Fig. 1.8 Mechanism of stereospecific polymerization of methyl methacrylate

is the chirality of the metal center caused by the ligand structure [16]. The selection of the prochiral faces with these chiral centers are named chain-end control and enantiomorphic-site control (or catalytic-site control), respectively (Fig. 1.7). If these chiral center continuously select the same prochiral face (*re–re–re*●●● or *si–si–si*●●●), isotactic polymer is produced. Whereas syndiotactic polymer is produced by alternating selection of *re* and *si* faces.

It should be noted that certain metallocene catalysts also conduct the stereospecific polymerization of methyl methacrylate and its derivatives. In this case, the active species is a metal enolate, and the configuration of the chiral carbon induced in the main chain is determined by the selection of the prochiral faces of the enolate (Fig. 1.8).

1.3.4 Polymerization Mechanism and Microtacticity

1.3.4.1 Chain-End Control

In a chain-end controlled mechanism, the chiral carbon at the propagation chain-end selects the prochiral face of incoming monomer. Thus, if the probability that

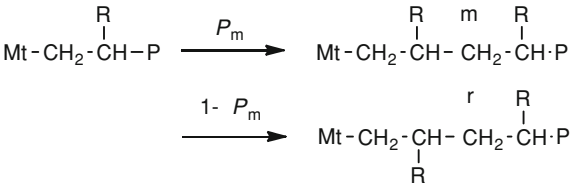

Fig. 1.9 Stereospecific polymerization by a chain-end control: the case of 1,2-insertion is shown

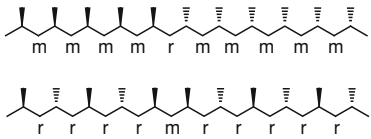

Fig. 1.10 Characteristic stereodefects formed by a chain-end controlled mechanism

the chain-end carbon selects the prochiral face to induce the same chirality is set to P_m, P_m is the probability of m diad formation. The probability of r diad formation P_r equals to $(1 - P_m)$: $P_m > 0.5$ and $P_m < 0.5$ indicate isotactic-specific and syndiotactic-specific polymerization (Fig. 1.9). In the case of $P_m = 0.5$, statistically atactic polymer is produced.

P_m (P_r) is independent of the proceeding diad, and the distribution of m and r in the polymer obeys a Bernullian statics. Thus, the probability of any stereo sequence is expressed by one probability P_m or P_r. For example, diad and triad are expressed by P_m as follows [17].

$$[m] = P_m; \quad [r] = 1 - P_m \tag{1.23}$$

$$[mm] = P_{m^2}; \quad [mr] = [rm] = 2P_m(1 - P_m); \quad [rr] = (1 - P_m)^2 \tag{1.24}$$

Thus, the steric triads of the polymer produced by a chain-end controlled mechanism satisfy the following equation.

$$4[mm]\,[rr]/[mr]^2 = 1 \tag{1.25}$$

In the isotactic-specific polymerization by a chain-end controlled mechanism, when the prochiral face is miss-selected, the chirality of the chain-end carbon is inverted and the opposite prochiral face is successively selected. Hence, the isolated r diad in m sequence is the characteristic stereodefect. Whereas, the isolated m diad in r sequence is the characteristic stereodefect in the syndiotactic-specific polymerization by a chain-end controlled mechanism (Fig. 1.10).

The selectivity of the prochiral faces is not high in a chain-end controlled mechanism, because the coordination of the monomer to the metal (Mt) is regulated by the chiral carbon which located one σ-bond away in the case of 2,1-insertion, Mt–C*H(R)–P, or two σ-bond away in the case of 1,2-insertion, Mt–C–C*H(R)–P. Thus a low temperature is necessary for stereospecific polymerization by a chain-end controlled mechanism.

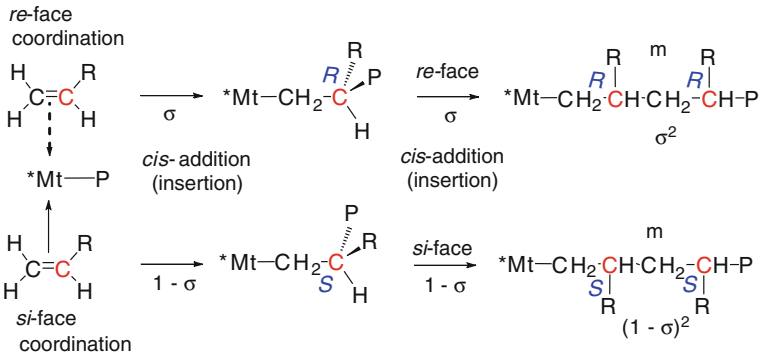

Fig. 1.11 Formation of m diad by an enantiomorphic-site controlled mechanism on *re*-face preferential site

1.3.4.2 Enantiomorphic-Site Control

In an enantiomorphic-step controlled mechanism, a chiral metal center selects the prochiral face of coordinating monomer. Thus, if the probability that the metal center selects one of the prochiral faces is set to σ, steric diad and triad are expressed as follows [18] (Fig. 1.11).

$$[\mathrm{m}] = [RR] + [SS] = \sigma^2 + (1-\sigma)^2 \tag{1.26}$$

$$[\mathrm{r}] = [RS] + [SR] = 2\sigma(1-\sigma) \tag{1.27}$$

$$[\mathrm{mm}] = [RRR] + [SSS] = \sigma^3(1-\sigma)^3 \tag{1.28}$$

$$\begin{aligned}[\mathrm{mr}] = [\mathrm{rm}] &= [RRS] + [SSR] + [RSS] + [SRR] \\ &= 2\sigma^2(1-\sigma) + 2\sigma(1-\sigma)^2\end{aligned} \tag{1.29}$$

$$[\mathrm{rr}] = [RSR] + [SRS] = \sigma^2(1-\sigma) + \sigma(1-\sigma)^2 \tag{1.30}$$

Thus,

$$[\mathrm{mr}] : [\mathrm{rr}] = 2 \ : \ 1 \tag{1.31}$$

Even if the metal center accidentally selects the other prochiral face with the probability of $1 - \sigma$, the original prochiral face of the successive monomer is selected with the probability of σ by the stereorigid chiral metal center. Therefore rr diad in m sequences is the characteristic stereodefect in the isotactic polymer formed by an enantiomorphic-site controlled mechanism: the steric pentad satisfy the following relation; [mmmr]:[mmrr]:[mrrm] = 2:2:1.

Syndiotactic polymer by an entiomorphic-site controlled mechanism is produced when the chiral active center isomerizes to the antipode after each monomer

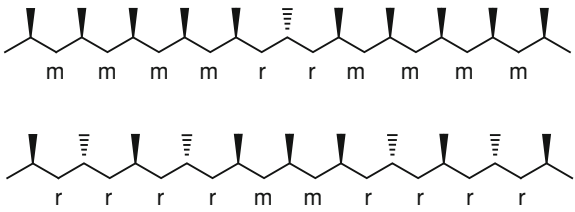

Fig. 1.12 Characteristic stereodefects formed by an enantiomorphic-site controlled mechanism

insertion. Consequently, *re*- and *si*-face are alternating selected to form syndiotactic polymer. If the *re*-face selectivity of the chiral metal center is set to λ, the *si*-face selectivity of the antipode is also λ. Thus, the following relations are derived in diad and triad.

$$[\mathrm{r}] = \lambda^2 + (1-\lambda)^2, \quad [\mathrm{m}] = 2\lambda(1-\lambda) \tag{1.32}$$

$$[\mathrm{rr}] = \lambda^3 + (1-\lambda)^3 \tag{1.33}$$

$$[\mathrm{mr}] = [\mathrm{rm}] = 2\lambda^2(1-\lambda) + 2\lambda(1-\lambda)^2 \tag{1.34}$$

$$[\mathrm{mm}] = \lambda^2(1-\lambda) + \lambda(1-\lambda)^2 \tag{1.35}$$

Thus,

$$[\mathrm{rm}] : [\mathrm{mm}] = 2 \ : \ 1 \tag{1.36}$$

If the chiral center which prefers *re*-face occasionally selects *si*-face or vice versa with the probability of $1 - \lambda$, the same prochiral face is consecutively selected in three times to form isolated mm triad in syndiotactic sequence (Fig. 1.12). When the chiral center isomerizes to the antipode without monomer insertion, the same prochiral face is consecutively selected in two times to form isolated m diad in syndiotactic sequence. This stereodefect is the same with that formed in a syndiotactic polymer by a chain end-controlled mechanism.

1.3.4.3 Polypropylene Obtained by Ziegler–Natta Catalysts

Isotactic polypropylene is currently produced by Ti-based heterogeneous Ziegler Natta catalysts. The polypropylenes obtained can be fractionated by boiling heptane. The weight fraction of heptane-insoluble part, called as isotactic index (I.I.), is used for evaluating the isotactic-specificity of catalyst. We should keep in mind that I.I. is the ratio of non-stereospecific and stereospecific sites and does not indicate the selectivity of prochiral face at an isotactic-specific site. Kakugo et al. fractionated isotactic polypropylenes obtained with β-$TiCl_3$–$AlEt_2Cl$ (mmmm = 94.5 %, $\bar{M}_n$ = 252,000) and δ-$TiCl_3$–$AlEt_2Cl$ (mmmm = 97.5 %, $\bar{M}_n$ = 315,000) by an elution column technique, where the temperature of elute was gradually increased [19]. They analyzed each fraction by GPC, DSC and $^{13}C\{^1H\}$ NMR in

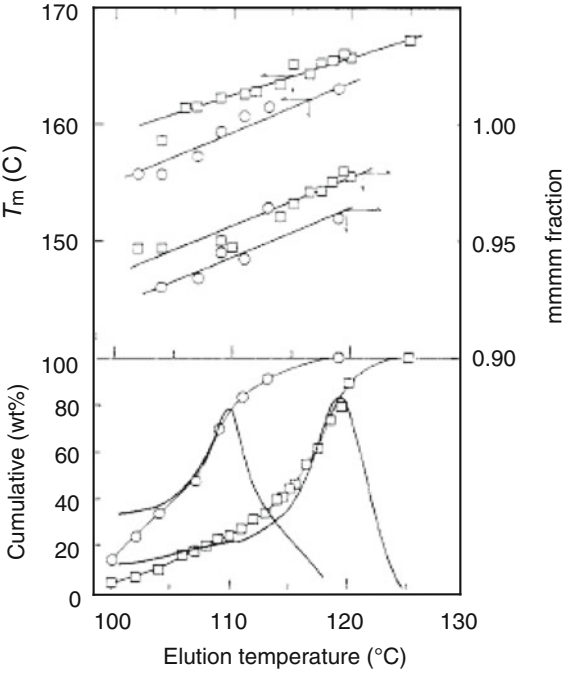

Fig. 1.13 Cumulative and differential fractionation curves, and the melting temperatures and the isotactic pentads (mmmm) of the fractions. Catalyst systems: (○)β-$TiCl_3$-Et_2AlCl; (□)δ-$TiCl_3$-Et_2AlCl [19]

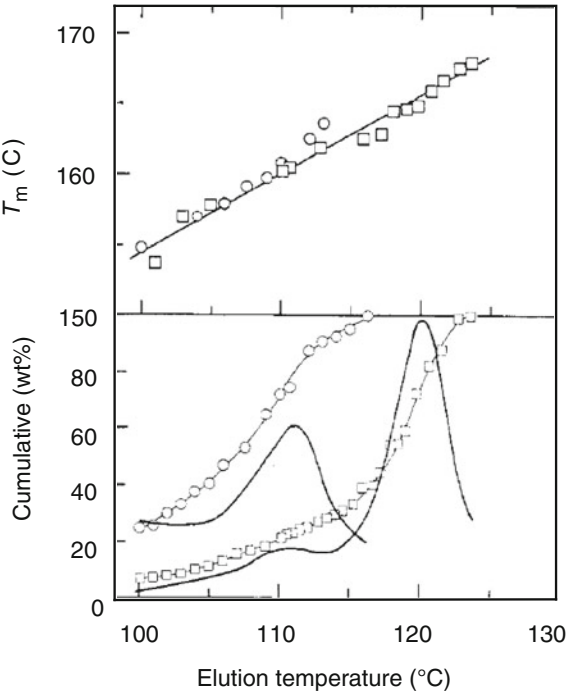

Fig. 1.14 Cumulative and differential fractionation curves, and the melting temperatures of each fraction. Catalyst systems: $MgCl_2$-supported Ti–Et_3Al with (□) and without (○) methyl *p*-toluate [19]

detail and displayed the microtacticity distribution of the isotactic polypropylenes as shown in Fig. 1.13, which clearly indicates that the active site of δ-$TiCl_3$ is more isotactic-selective than that of β-$TiCl_3$.

They applied this technique to investigate the additive effects of Lewis base on propylene polymerization with a $MgCl_2$-supported Ti-based catalyst and clarified that the addition of methyl *p*-toluate suppressed the formation of isotactic-selective site with low σ value and newly gave the isotactic-selective site with high *σ* value. (Fig. 1.14).

This technique is named Temperature Rising Elution Fractionation (TREF) and applied also for ethylene-based copolymers.

The microtacticity of heptane-soluble atactic polypropylene (Fig. 1.4a) was well-characterized by the combination of syndiotactic sequence with a chain-end controlled mechanism and isotactic sequence with an enantiomorphic-site controlled mechanism, suggesting that the polypropylenes should have a stereoblock structure [20].

1.4 Copolymer and Copolymerization

1.4.1 Structure of Copolymers

If we consider a linear copolymer consisted of two different monomers, M_1 and M_2, three typical structures can be considered; random, alternate and block structures as shown in Fig. 1.15. Random copolymer is the copolymer in which the comonomer sequence distribution obeys a Bernoullian statics. Copolymer in which the comonomer sequence distribution obeys a known statistical law is named statistical copolymer, and expressed by poly(M_1-*stat*-M_2). Although random copolymer is a special case of statistical copolymers, the word "random" is not clearly distinguished from "statistical" and frequently used for the copolymer where comonomer composition is controlled freely.

1.4.2 Copolymerization

We can synthesize homopolymers with various physical properties by controlling molecular weight, molecular weight distribution and stereoregularity. If we can introduce second monomer freely at the place we want as shown in Fig. 1.15, the kinds of polymers obtained are almost unlimited. Thus, copolymerization is very important to synthesize a wide variety of polymers from a few limited monomers. Polyolefin is a good example. Crystallinity of polyethylene is controlled by introducing 1-alkene (linear low density polyethylene, LLDPE), and elastomer is obtained by copolymerization of ethylene and propylene (EPR). Crystallinity of isotactic polypropylenes is also controlled by introducing a small amount of ethylene or 1-butene, and the product is called random polypropylene.

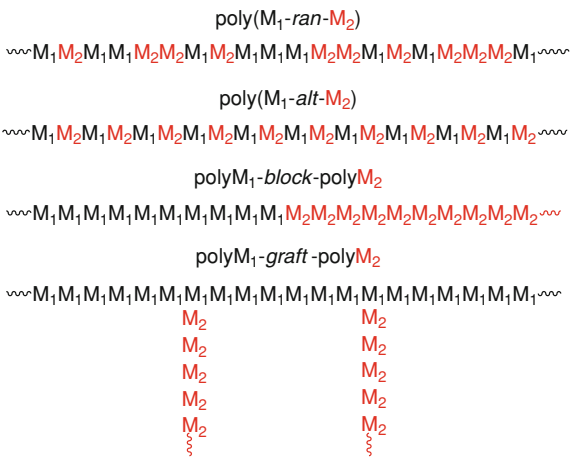

Fig. 1.15 Structures of copolymers, poly(M1-*co*-M2) or copoly(M1/M2)

1.4.2.1 Kinetic Treatment

We consider binary copolymerization of two monomers, M_1 (ethylene) and M_2 (propylene or 1-alkene) as the simplest case [21, 22]. The copolymerization consists of initiation, propagation, chain transfer and/or termination reaction. When the copolymerization proceeds in a steady state to produce high molecular weight copolymer, we can concentrate on the propagation reaction to consider the comonomer composition in the copolymer. If the insertion of M_2 is regioselective and the reactivity of the active species is determined by the last inserted monomer unit, the propagation reaction involves the following four reactions, where the catalytic center is shown with Ti for descriptive purposes. It should be noted that the system should be treated as the ternary copolymerization consisted of M_1, 1,2-inserted M_2 and 2,1-inserted M_2 units when the insertion of M_2 is not regioselective.

$$\sim\!\!\sim M_1\text{–Ti} + M_1 \xrightarrow{k_{11}} \sim\!\!\sim M_1M_1\text{–Ti} \tag{1.37}$$

$$\sim\!\!\sim M_1\text{–Ti} + M_2 \xrightarrow{k_{12}} \sim\!\!\sim M_1M_2\text{–Ti} \tag{1.38}$$

$$\sim\!\!\sim M_2\text{–Ti} + M_1 \xrightarrow{k_{21}} \sim\!\!\sim M_2M_1\text{–Ti} \tag{1.39}$$

$$\sim\!\!\sim M_2\text{–Ti} + M_2 \xrightarrow{k_{22}} \sim\!\!\sim M_2M_2\text{–Ti} \tag{1.40}$$

Here k_{ij} is the rate constant of step ij, and the subscripts 1 and 2 refer to M_1 and M_2, respectively.

Thus the consumption rates of M_1 and M_2 are

$$\frac{d[M_1]}{dt} = k_{11}[C_1^*][M_1] + k_{12}[C_1^*][M_2] \tag{1.41}$$

$$\frac{d[M_2]}{dt} = k_{21}[C_2^*][M_1] + k_{22}[C_2^*][M_2] \tag{1.42}$$

Here $[C_1^*]$ and $[C_2^*]$ are the concentration of M_1-inserted and M_2-inserted active species, respectively. The ratio of Eqs. 1.41 and 1.42 gives the ratio of the two monomers incorporated in the copolymer:

$$\frac{d[M_1]}{d[M_2]} = \frac{k_{11}[C_1^*][M_1] + k_{12}[C_1^*][M_2]}{k_{21}[C_2^*][M_1] + k_{22}[C_2^*][M_2]} \tag{1.43}$$

The steady-state approximation is applied for $[C_1^*]$ and $[C_2^*]$ to give

$$k_{12}[C_1^*][M_2] = k_{21}[C_2^*][M_1] \tag{1.44}$$

or

$$\frac{[C_1^*]}{[C_2^*]} = \frac{k_{21}[M_1]}{k_{12}[M_2]} \tag{1.45}$$

Combining Eqs. 1.43 and 1.45 yields comonomer composition equation or copolymerization equation:

$$\frac{d[M_1]}{d[M_2]} = \frac{[M_1]\, r_1[M_1] + [M_2]}{[M_2]\, [M_1] + r_2[M_2]} \tag{1.46}$$

Here r_1 and r_2 are monomer reactivity ratios defined by Eqs. 1.47 and 1.48, indicating the relative activity of each monomer on the M_1-inserted and the M_2-inserted Ti species, respectively.

$$r_1 = \frac{k_{11}}{k_{12}} \tag{1.47}$$

$$r_2 = \frac{k_{22}}{k_{21}} \tag{1.48}$$

Substitute $[M_1]/[M_2]$ and $d[M_1]/d[M_2]$ with F and f in Eq. 1.46:

$$f = \frac{F(r_1F + 1)}{F + r_2} \tag{1.49}$$

Rearrange Eq. 1.49 to give

$$\frac{F(f-1)}{f} = \frac{r_1F^2}{f} - r_2 \tag{1.50}$$

Thus, r_1 and r_2 can be evaluated from the slope and intercept of the $F(f-1)/f$ versus F^2/f plot in the copolymerization with various comonomer feed ratios. This method is known as a Finemann–Ross plot [23]. Since Eq. 1.50 is derived on condition that the copolymerization proceeds in a steady state, the conversion of each monomer should be kept low in order to determine the r_1 and r_2 values precisely with this method.

The values of r_1 and r_2 are the fundamental parameters for describing a copolymerization system, and hence characterizing the copolymerization ability of a catalyst. r_i is the ratio of two propagation rate constants involving M_i-inserted active species: the ratio always compares the propagation rate constant for the same monomer inserting the active species relative to the propagation rate constant for the other monomer. If $r_i > 1$, M_i-inserted active species preferentially inserts the same monomer M_i; if $r_i < 1$, M_i-inserted active species preferentially inserts the other monomer; if $r_i = 0$, M_i-inserted active species does not insert the same monomer. Thus, the product of monomer reactivity ratios, $r_1 \bullet r_2$, is indicative for the structure of the copolymer obtained: $r_1 \bullet r_2 > 1$, blocky; $r_1 \bullet r_2 = 1$, random; $r_1 \bullet r_2 = 0$, alternate.

1.4.2.2 Statistical Treatment

In Sect. 1.4.2.1, we noted that the nature of a steady-state copolymerization system is characterized by r_1 and r_2 which are determined from the comonomer compositions of copolymers [24]. The analysis of monomer sequence distribution in a copolymer gives more detailed information on the copolymerization because each monomer sequence reflects each propagation step.

We can analyze the comonomer composition and the monomer sequence distribution of a copolymer by a probabilistic method on the assumption that the copolymer is statistically stationary. In a binary copolymer which has high molecular weight enough to neglect the chain-end effects, any monomer unit possesses the preceding and succeeding monomer units (M_1 or M_2), and the probability that the mth monomer unit is a given monomer unit (M_1 or M_2) is independent of m and equal to the probability of the randomized monomer unit. When a copolymer satisfies these conditions, the sequence distribution of

monomer is referred to as statistical stationarity. A certain limited length of monomer sequence also satisfies these conditions, and the following quantity can be defined.

$$P_n\{\mathrm{M}_i\mathrm{M}_j\ldots\mathrm{M}_v\} = \text{the probability that a randomized monomer sequence with } n \text{ monomer units } (n \text{ length}) \text{ is a certain monomer sequence } \mathrm{M}_i\mathrm{M}_j\ldots\mathrm{M}_v (i, j, \ldots, v = \text{ 1 or 2}).$$

For example, possible sequences are as follows.

$n = 1$, M_1 and M_2;
$n = 2$, $\mathrm{M}_1\mathrm{M}_1$, $\mathrm{M}_1\mathrm{M}_2$, $\mathrm{M}_2\mathrm{M}_1$ and $\mathrm{M}_2\mathrm{M}_2$
$n = 3$, $\mathrm{M}_1\mathrm{M}_1\mathrm{M}_1$, $\mathrm{M}_1\mathrm{M}_1\mathrm{M}_2$, $\mathrm{M}_1\mathrm{M}_2\mathrm{M}_1$, $\mathrm{M}_1\mathrm{M}_2\mathrm{M}_2$, $\mathrm{M}_2\mathrm{M}_1\mathrm{M}_1$, $\mathrm{M}_2\mathrm{M}_1\mathrm{M}_2$, $\mathrm{M}_2\mathrm{M}_2\mathrm{M}_1$ and $\mathrm{M}_2\mathrm{M}_2\mathrm{M}_2$.

In general, 2^n kinds of sequences are present in the sequence with n length. According to the definition of $P_n\{\mathrm{M}_i\mathrm{M}_j\ldots\mathrm{M}_v\}$, $P_1\{\mathrm{M}_i\}$, $P_2\{\mathrm{M}_i\mathrm{M}_j\}$ and $P_3\{\mathrm{M}_i\mathrm{M}_j\mathrm{M}_k\}$ are the existence probabilities or mole fractions of the corresponding monomer, diad and triad, respectively.

For given n, the summation of the probabilities of all the possible monomer sequences is unit. Thus,

$$P_1\{\mathrm{M}_1\} + P_1\{\mathrm{M}_2\} = 1 \tag{1.51}$$

$$P_2\{\mathrm{M}_1\mathrm{M}_1\} + P_2\{\mathrm{M}_1\mathrm{M}_2\} + P_2\{\mathrm{M}_2\mathrm{M}_1\} + P_2\{\mathrm{M}_2\mathrm{M}_2\} = 1 \tag{1.52}$$

If a certain monomer sequence with n length is defined as $S^{(n)}$,

$$\begin{aligned} P_n\left\{S^{(n)}\right\} &= P_{n+1}\left\{S^{(n)}\mathrm{M}_1\right\} + P_{n+1}\left\{S^{(n)}\mathrm{M}_2\right\} \\ &= P_{n+1}\left\{\mathrm{M}_1S^{(n)}\right\} + P_{n+1}\left\{\mathrm{M}_2S^{(n)}\right\} \end{aligned} \tag{1.53}$$

In the case of $S^{(1)} = \mathrm{M}_1$

$$P_1\{\mathrm{M}_1\} = P_2\{\mathrm{M}_1\mathrm{M}_1\} + P_2\{\mathrm{M}_1\mathrm{M}_2\} = P_2\{\mathrm{M}_1\mathrm{M}_1\} + P_2\{\mathrm{M}_2\mathrm{M}_1\} \tag{1.54}$$

Thus,

$$P_2\{\mathrm{M}_1\mathrm{M}_2\} = P_2\{\mathrm{M}_2\mathrm{M}_1\} \tag{1.55}$$

Equation 1.55 corresponds to the steady-state approximation in the kinetic treatment, Eq. 1.44.

Generally, the substitution of $S^{(n)} = \mathrm{M}_i^n$ for an arbitrary integer $n \geq 1$ in Eq. 1.53 yields:

$$\begin{aligned} P_{n+1}\left\{\mathrm{M}_1^n\mathrm{M}_2\right\} &= P_{n+1}\left\{\mathrm{M}_2\mathrm{M}_1^n\right\} \\ P_{n+1}\left\{\mathrm{M}_2^n\mathrm{M}_1\right\} &= P_{n+1}\left\{\mathrm{M}_1\mathrm{M}_2^n\right\} \end{aligned} \tag{1.56}$$

$P_2\{\mathrm{M}_1\mathrm{M}_2\}$ or $P_2\{\mathrm{M}_2\mathrm{M}_1\}$ is developed with Eq. 1.53 as follows:

$$\begin{aligned} P_2\{\mathrm{M}_2\mathrm{M}_1\} &= P_3\{\mathrm{M}_2\mathrm{M}_1\mathrm{M}_2\} + P_3\{\mathrm{M}_2\mathrm{M}_1\mathrm{M}_1\} \\ &= P_3\{\mathrm{M}_2\mathrm{M}_1\mathrm{M}_2\} + P_4\{\mathrm{M}_2\mathrm{M}_1\mathrm{M}_1\mathrm{M}_2\} + P_4\{\mathrm{M}_2\mathrm{M}_1\mathrm{M}_1\mathrm{M}_1\} \\ &= \cdots \\ &= \sum_{n=1}^{\infty} P_n + 2\{\mathrm{M}_2\mathrm{M}_1^n\mathrm{M}_2\} + \lim_{n\to\infty} P_{n+2}\{\mathrm{M}_2\mathrm{M}_1^{n+1}\} \end{aligned} \tag{1.57}$$

Since the second term is zero, the following equation is obtained.

$$\begin{aligned} P_2\{\mathrm{M}_1\mathrm{M}_2\} &= P_2\{\mathrm{M}_2\mathrm{M}_1\} \\ &= \sum_{n=1}^{\infty} P_{n+2}\{\mathrm{M}_2\mathrm{M}_1^n\mathrm{M}_2\} + \sum_{n=1}^{\infty} P_{n+2}\{\mathrm{M}_1\mathrm{M}_2^n\mathrm{M}_1\} \end{aligned} \tag{1.58}$$

$P_{n+2}\{\mathrm{M}_2\mathrm{M}_1^n\mathrm{M}_2\}$ (or $P_{n+2}\{\mathrm{M}_1\mathrm{M}_2^n\mathrm{M}_1\}$) is the existence probability of the M_1 (or M_2) homo sequence with n length, which is named as "run with n length" according to Harwood and Ritchey [25]. Equation 1.58 implies that $P_2\{\mathrm{M}_1\mathrm{M}_2\}$ or $P_2\{\mathrm{M}_2\mathrm{M}_1\}$ equals to the number fraction of total M_1 run or total M_2 run. We can understand this relation intuitively from the statistical stationarity of copolymer: an infinite number of M_1 run and M_2 run are alternatively connected with $\mathrm{M}_1\mathrm{M}_2$ and $\mathrm{M}_2\mathrm{M}_1$ diads.

$P_2\{\mathrm{M}_1\mathrm{M}_2\}$ and $P_2\{\mathrm{M}_2\mathrm{M}_1\}$ are the important quantities which characterize monomer sequence distribution in copolymer. Run number R is defined as a summation of the total number of run per 100 monomer units. That is:

$$R = 100(P_2\{\mathrm{M}_1\mathrm{M}_2\} + P_2\{\mathrm{M}_2\mathrm{M}_1\}) = 200P_2\{\mathrm{M}_1\mathrm{M}_2\} = 200P_2\{\mathrm{M}_2\mathrm{M}_1\} \tag{1.59}$$

Since $\mathrm{M}_1\mathrm{M}_2$ and $\mathrm{M}_2\mathrm{M}_1$ cannot be distinguished in vinyl polymers and $P_2\{\mathrm{M}_1\mathrm{M}_2\} = P_2\{\mathrm{M}_2\mathrm{M}_1\}$ under the stationary conditions, $\mathrm{M}_1\mathrm{M}_2$ represents the both hetero diads. It should be noted that all the equations containing $P_2\{\mathrm{M}_1\mathrm{M}_2\}$ or $P_2\{\mathrm{M}_2\mathrm{M}_1\}$ in this chapter is true by dividing those value by 2 for vinyl polymers.

1.4.2.3 Monomer Sequence Distribution and Copolymerization Mechanism

For simplicity, we postulate the conditions that monomer concentration, comonomer composition and monomer sequence distribution are practically constant [24]. When the diad probability of a certain copolymer is given, the number-average

length of M_1 run (l_1) or M_2 run (l_2) can be calculated irrespective of the copolymerization mechanism:

$$l_1 = P_1\{M_1\}/P_2\{M_1M_2\} = 200P_1\{M_1\}/R \tag{1.60}$$

$$l_2 = P_1\{M_2\}/P_2\{M_2M_1\} = 200P_1\{M_2\}/R \tag{1.61}$$

When M_1 and M_2 are independently (or perfectly randomly) distributed, it is said that the distribution of M_1 and M_2 obeys Bernoulli trials, where the following relation is satisfied: $P_2\{M_1M_2\} = P_2\{M_2M_1\} = P_1\{M_1\}\,P_2\{M_2\}$; thus, $l_{1,\,\mathrm{random}} = 1/P_1\{M_2\}$, $l_{2,\,\mathrm{random}} = 1/P_1\{M_1\}$, $R_{\mathrm{random}} = 200\;P_1\{M_1\}\;P_1\{M_2\}$. Persistence ratio ρ for a parameter characterizing the block nature of a given copolymer is defined by the following equation [26]:

$$\rho = \frac{R_{\mathrm{random}}}{R} = \frac{l_1}{l_{1,\,\mathrm{random}}} = \frac{l_2}{l_{2,\,\mathrm{random}}} = \frac{2P_1\{M_1\}P_1\{M_2\}}{P_2\{M_1M_2\} + P_2\{M_2M_1\}} \tag{1.62}$$

It is apparent that $\rho = 1$ indicates Bernoulli trials, and $\rho > 1$ or $\rho < 1$ imply more blocky or more alternating than Bernoulli trials, respectively.

In general, when the probability that a certain monomer unit or a certain monomer sequence distribution occurs is dependent of the preceding N monomer units but independent of further preceding monomer units ($N + 1$ or more), the probability process is said to obey Nth-order Markov chain: $N = 0$ is equal to Bernoulli trials. First-order Markov chain ($N = 1$) is also called simple Markov chain. In Nth-order Markovian process, any monomer sequence $S^{(n)}$ satisfies the following equation:

$$\frac{P_{m+N+n}\{U^{(m)}V^{(N)}S^{(n)}\}}{P_{m+N}\{U^{(m)}V^{(N)}\}} = \frac{P_{N+n}\{V^{(N)}S^{(n)}\}}{P_{m+N}\{V^{(N)}\}} \tag{1.63}$$

Here, $V^{(N)}$ is the monomer sequence preceding $S^{(n)}$ with N length, and $U^{(m)}$ is any monomer sequence preceding $V^{(N)}$ with m length. The right-hand side of Eq. 1.63 is the conditional probability that monomer sequence $S^{(n)}$ occurs after a given monomer sequence $V^{(N)}$. Similarly, the left-hand side Eq. 1.63 is the conditional probability that monomer sequence $S^{(n)}$ occurs after a given monomer sequence $U^{(m)}V^{(N)}$. When the integer N which satisfies Eq. 1.63 does not exist, the probability process is said to be non-Malkov chain.

In order to correlate monomer sequence distribution with copolymerization mechanism, we define the conditional probability $P_{ijk\ldots\,\mathrm{vw}}$ ($i, j, k, \ldots, v, w = 1$ or 2) that the monomer unit M_w occurs after the monomer sequence $M_iM_j\ldots M_v$ in Nth-order Markov chain ($N \geq 0$).

$$P_{ijk\cdots vw} = \frac{P_{n+1}\{M_iM_jM_k\ldots M_vM_w\}}{P_n\{M_iM_jM_k\ldots M_v\}} \tag{1.64}$$

Since $M_w = M_1$ or M_2, Eqs. 1.53 and 1.64 give

$$P_{ijk\cdots v1} + P_{ijk\cdots v2} = 1 \tag{1.65}$$

The existence probability of a certain monomer sequence is expressed from Eq. 1.64:

$$\begin{aligned} &P_n\{M_iM_jM_k\ldots M_uM_v\} \\ &\quad = P_1\{M_i\} \cdot \frac{P_2\{M_iM_j\}}{P_1\{M_i\}} \cdot \frac{P_3\{M_iM_jM_k\}}{P_2\{M_iM_j\}} \cdot \cdots \cdot \frac{P_n\{M_iM_jM_k\ldots M_uM_v\}}{P_{n-1}\{M_iM_jM_k\ldots M_u\}} \\ &\quad = P_1\{M_i\}P_{ij}P_{ijk}\cdots P_{ijk}\cdots \end{aligned} \tag{1.66}$$

Here, $P_1\{M_i\}$ is the probability that the randomly selected monomer unit is M_i; P_{ij}, P_{ijk} and $P_{ijk\ldots\ uv}$ are the conditional probabilities that M_j, M_k and M_v occur on condition that the preceding monomer sequences are M_i, M_iM_j and $M_iM_jM_k\ldots M_u$, respectively. Equation 1.66 indicates that $P_n\{M_iM_jM_k\ldots M_v\}$ is given by the product of these n probabilities.

General Eq. 1.66 is simplified by deciding the N value of Nth-order Malkov chain according to a given copolymerization mechanism and can be calculated specifically. For example, the existence probability of the sequence of continuous n M_1 units, $P_{n+2}\{M_2M_1^nM_2\}$ is calculated with a given N value:
when $N = 0$

$$\begin{aligned} &P_{n+2}\{M_2M_1^nM_2\} = (P_1\{M_2\})^2(P_1\{M_1\})^n = P_2^2P_1^n = (1-P_1)^2P_1^n \\ &(\because P_1\{M_1\} + P_1\{M_2\} = 1, P_1\{M_1\} = P_1, P_1\{M_2\} = P_2) \end{aligned} \tag{1.67a}$$

when $N = 1$

$$P_{n+2}\{M_2M_1^nM_2\} = P_1\{M_2\}P_{21}P_{11}^{n-1}P_{12} = P_2\{M_2M_1\}P_{11}^{n-1}P_{12} \tag{1.67b}$$

when $N = 2$

$$\begin{aligned} P_{n+2}\{M_2M_1^nM_2\} &= P_1\{M_2\}P_{21}P_{211}P_{111}^{n-2}P_{112} \\ &= P_2\{M_2M_1\}P_{211}^{n-1}P_{112}(n \geq 2) \end{aligned} \tag{1.67c}$$

$$P_3\{M_2M_1M_2\} = P_1\{M_2\}P_{21}P_{212} = P_2\{M_2M_1\}P_{212}(n = 1) \tag{1.67d}$$

The order of Malkov chain N can be experimentally evaluated by Eq. 1.63 when the existence probabilities at least with $N + 2$ length are independently given. The corresponding conditional probabilities can be directly obtained by Eq. 1.64 from the ratio of the existence probabilities of $N + 1$ length and N. The following relations are available when $N = 1$, 2, or 3, and i, j, k, $l = 1$ or 2:

when $N = 0$

$$\frac{P_2\{\mathrm{M}_j\mathrm{M}_i\}}{P_1\{\mathrm{M}_j\}} = P_1\{\mathrm{M}_i\} = P_i \tag{1.68a}$$

when $N = 1$

$$\frac{P_3\{\mathrm{M}_k\mathrm{M}_i\mathrm{M}_j\}}{P_2\{\mathrm{M}_k\mathrm{M}_i\}} = \frac{P_2\{\mathrm{M}_i\mathrm{M}_{ij}\}}{P_1\{\mathrm{M}_i\}} = P_{ij} \tag{1.68b}$$

when $N = 2$

$$\frac{P_4\{\mathrm{M}_l\mathrm{M}_i\mathrm{M}_j\mathrm{M}_k\}}{P_3\{\mathrm{M}_l\mathrm{M}_i\mathrm{M}_j\}} = \frac{P_3\{\mathrm{M}_i\mathrm{M}_j\mathrm{M}_k\}}{P_2\{\mathrm{M}_i\mathrm{M}_j\}} = P_{ijk} \tag{1.68c}$$

The copolymer of which monomer sequences do not satisfy these relations is *N*th-order Malkov chain of $N \geq 3$ or non-Malkov chain.

Above discussion implies that we can fully characterize monomer sequence distribution of a given copolymer obtained with a low monomer conversion by the probabilistic method (without any kinetic parameter) if we can determine N of Malkov chain and all the existence probabilities of the monomer sequences with $N + 1$ length: the existence probabilities of monomer sequences below N length are determined by Eq. 1.53 and the conditional probabilities are determined by either Eq. 1.64 or 1.68a. Hereafter, we will take the copolymerization described in Sect. 1.4.2.1 as an example and consider how the conditional probabilities, comonomer composition and monomer sequence distribution are correlated with given kinetic parameters and monomer concentrations.

$$P_{12} = \frac{k_{12}[C_1^*][\mathrm{M}_2]}{k_{11}[C_1^*][\mathrm{M}_1] + k_{12}[C_1^*][\mathrm{M}_2]} = \frac{1}{1 + r_1 x} = 1 - P_{11} \tag{1.69a}$$

$$P_{21} = \frac{k_{21}[C_2^*][\mathrm{M}_1]}{k_{22}[C_2^*][\mathrm{M}_2] + k_{21}[C_2^*][\mathrm{M}_1]} = \frac{1}{1 + r_2/x} = 1 - P_{22} \tag{1.69b}$$

Here, $r_1 = k_{11}/k_{12}$, $r_2 = k_{22}/k_{21}$, $x = [\mathrm{M}_1]/[\mathrm{M}_2]$.

Copolymer composition equation is obtained from Eqs. 1.55 and 1.66:

$$P_1\{\mathrm{M}_1\}P_{12} = P_1\{\mathrm{M}_2\}P_{21}$$

thus,

$$P_1\{\mathrm{M}_1\}/P_1\{\mathrm{M}_2\} = P_{21}/P_{12} \tag{1.70a}$$

or from Eqs. 1.51 and 1.70a:

$$P_1\{M_1\} = P_{21}/(P_{12} + P_{21}), P_1\{M_2\} = P_{12}/(P_{12} + P_{21}) \tag{1.70b}$$

Substituting Eq. 1.69a, b, into Eq. 1.70a, we obtain comonomer composition equation (Eq. 1.46).

The existence probability of a certain monomer sequence is defined by P_{ij}. For example,

$$P_2\{M_1M_1\} = P_{21}P_{11}/(P_{12} + P_{21}) \tag{1.71a}$$

$$P_2\{M_1M_2\} = P_2\{M_2M_1\} = R/200 = P_{12}P_{21}/(P_{12} + P_{21}), \tag{1.71b}$$

$$P_2\{M_2M_2\} = P_{12}P_{22}/(P_{12} + P_{21}) \tag{1.71c}$$

$$P_3\{M_1M_1M_1\} = P_{21}P_{11}^2/(P_{12} + P_{21}) \tag{1.71d}$$

$$P_3\{M_1M_1M_2\} = P_3\{M_2M_1M_1\} = P_{21}P_{11}P_{12}/(P_{12} + P_{21}) \tag{1.71e}$$

$$P_3\{M_2M_1M_2\} = P_{21}P_{12}^2/(P_{12} + P_{21}) \tag{1.71f}$$

$$P_{n+1}\left\{M_1^nM_2\right\} = P_{n+1}\left\{\ M_2M_1^n\right\} = P_{21}P_{12}P_1^{n-1}\ {}_1/(P_{12} + P_{21}) \tag{1.71g}$$

Persistence ratio ρ and the number-average length of M_i are obtained similarly by substituting conditional probabilities into each definitional identity.

$$\rho = 1/(P_{12} + P_{21}) \tag{1.72}$$

$$l_1 = 1/P_{12},\ l_2 = 1/P_{21} \tag{1.72}$$

Equations 1.71a–1.73 are converted to the functions of monomer reactivity ratios and monomer feed ratio. For example,

$$R = 200/(2 + r_1x + r_2/x) \tag{1.73}$$

$$\rho = \frac{1 + r_1r_2 + r_1x + r_2/x}{2 + r_1x + r_2/x} \tag{1.74}$$

$$l_1 = 1 + r_1x,\ l_2 = 1 + r_2/x \tag{1.75}$$

Equation 1.74 shows the relation between ρ and the product of monomer reactivity ratios, $r_1 \bullet r_2$: $r_1 \bullet r_2 = 1$, $\rho = 1$ (Bernoulli trials); $r_1 \bullet r_2 > 1$, $\rho > 1$ (more blocky than Bernoulli trials); $r_1 \bullet r_2 < 1$, $\rho < 1$ (more alternate than Bernoulli trials).

When daid probabilities are experimentally obtained, l_1 and l_2 are directly obtained by Eq. 1.60. Thus, Eq. 1.75 is important for determining monomer reactivity ratios and testing terminal model by the linear plot against x or $1/x$. The

direct evaluation of terminal model is to compare the probabilities of diad and triad which are experimentally obtained by Eq. 1.68b. For example,

$$\frac{P_3\{M_1M_1M_2\}}{P_2\{M_1M_1\}} = \frac{P_3\{M_2M_1M_2\}}{P_2\{M_2M_1\}} = \frac{P_2\{M_1M_2\}}{P_1\{M_1\}} = P_{12} = \frac{1}{1 + r_1 x} \tag{1.76}$$

If terminal model ($N = 1$) is confirmed, we can principally determine r_1 and r_2 from the diad probabilities of only one sample on condition that monomer feed ratio and comonomer composition are known.

$$\frac{P_2\{M1M1\}}{P_2\{M1M2\}} = \frac{k_{11}[C_1^*][M_1]}{k_{12}[C_1^*][M_2]} = r_1 x \tag{1.77}$$

$$\frac{P_2\{M_2M_2\}}{P_2\{M_2M_1\}} = \frac{k_{22}[C_2^*][M_2]}{k_{21}[C_2^*][M_1]} = r_2/x \tag{1.78}$$

Since M_1M_2 and M_2M_1 cannot be distinguished in olefin copolymers, r_1 and r_2 is obtained by the following equations using a half of the observed $P_2\{M_1M_2\}$ (= $P_2\{M_1M_2\}$) as described in Sect. 1.4.2.2.

$$r_1 = \frac{P_2\{M_1M_1\}}{P_2\{M_1M_2\}\ /2} \cdot \frac{1}{x} \tag{1.80}$$

$$r_2 = \frac{P_2\{M_2M_2\}}{P_2\{M_1M_2\}\ /2} \cdot x \tag{1.81}$$

1.4.2.4 Comonomer Composition Distribution

A majority of LLDPE are still produced with $MgCl_2$-supported Ti-based catalysts, although a variety of single-site catalysts has been developed. As described in Sect. 1.3.4.3, $MgCl_2$-supported Ti-based catalysts contain a several active species which are different in isotactic-selectivity. We can imagine that these active species possess different selectivity also for the copolymerization of ethylene and 1-alkene. Since the crystallinity of LLDPE decreases inversely with the 1-alkene content, we can fractionate LLDPE by the difference of crystallinity. Figure 1.16a displays the cross fractionation chromatogram (CFC), which is obtained by a combination of TREF and gel permeation chromatography (GPC), of the ethylene–1-butene copolymer obtained with a Ti-based $MgCl_2$-supported catalyst, indicating that the copolymer contain several fractions differing in crystallinity and molecular weight. In contrast, Fig. 1.16b indicates that the copolymer obtained with a

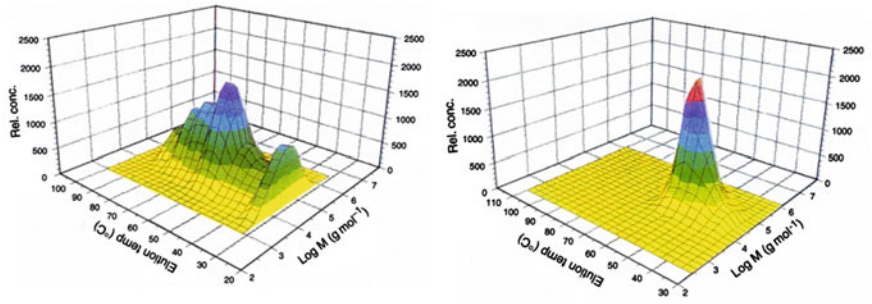

Fig. 1.16 CFC chromatograms of ethylene–1-butene copolymers obtained with **a** a heterogeneous Ziegler–Natta catalyst and **b** a homogeneous metallocene catalyst [27]

homogeneous metallocene catalyst is uniform both in molecular weight distribution and comonomer composition distribution.

In Sects. 1.4.2.1 and 1.4.2.3, we dealt with binary copolymerization with kinetic and probabilistic approaches, respectively, where we assume stationary conditions with one kind of active species. Thus, the methods are applied for single-site catalysts but not for multi-site catalysts. In the latter case, r_1 and r_2 obtained are apparent values.

1.5 Characteristics of Metallocene Catalysts

1.5.1 Activation Process of Metallocene

1.5.1.1 Active Species of Metallocene Catalyst

The research on Cp_2TiX_2–R_nAlCl_{3-n} systems started from the 1950s [9]. Since the systems showed the low activity only for ethylene polymerization, these systems were investigated as a model for studying the polymerization mechanism. The epoch-making discovery of MAO as a cocatalyst for a metallocene complex by Kaminsky and Sinn has enabled a practical use of metallocenes for olefin polymerization catalysts [8]. Their first paper on ethylene polymerization is entitled "*Halogenfreie lösliche Ziegler-Katalysatoren für die Ethylen-Polymerisation. Regelung des Molekulargewichts durch Wahl der Reaktionstemperatur*", where Cp_2MMe_2 (M = Ti, Zr) was activated by the mixture of Me_3Al and H_2O [28]. Their finding is important also at the point that halogen, which had been believed to be indispensable to show high activity for olefin polymerization, is essentially unnecessary.

The research on a metallocene catalyst progressed rapidly both from the fundamental and practical point of views after the discovery. The study on Cp_2TiX_2–R_nAlCl_{3-n} systems by a visible absorption spectrum, electrical conductivity,

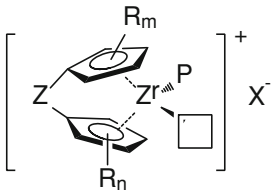

Fig. 1.17 Active species of group 4 metallocene catalyst

^{13}CNMR had presumed that the cationic Ti^{4+} species should be active for ethylene polymerization. Jordan et al. reported that the isolated cationic complex of Zr^{4+}, $[Cp_2ZrR(THF)][BPh_4]$(R = Me, CH_2Ph), conducted ethylene polymerization independently [29]. Furthermore, the formation of cationic Zr^{4+} species in a Cp_2ZrX_2–MAO system was confirmed by XPS [30] and solid CP MAS ^{13}CNMR [31]. It is no doubt that the active species of group 4 metallocene catalysts for olefin polymerization is coordinatively-unsaturated tetravalent alkyl cationic species (Fig. 1.17): the active species possesses a pseudo-tetrahedral structure where the bis(cyclopentadienyl) ligand of the precursor is retained and a growing polymer chain and a vacant site locate at *cis*-position. Namely, the structure of active species is determined by that of the metallocene precursor, which enables the molecular design of olefin polymerization catalysts.

1.5.1.2 Activation Method of Metallocene

It was considered that MAO should be necessary for metallocenes to show high activity in olefin polymerization [32]. The clarification of the active species has brought about various activation methods, which are classified as follows in the case of a dialkylmetallocene.

(1) One-electron oxidation

$$Cp_2ZrR_2 + Ag^+\left[B(C_6H_5)_4\right]^- \rightarrow [Cp_2ZrR]^+\left[B(C_6H_5)_4\right]^- + 1/2R_2 + Ag^0 \quad (1.82)$$

$$Cp_2ZrR_2 + \left[(MeCp)_2Fe\right]^+\left[B(C_6H_5)_4\right]^- \rightarrow [Cp_2ZrR]^+\left[B(C_6H_5)_4\right]^- + 1/2R_2 + (MeCp)_2Fe \quad (1.83)$$

$$Cp_2ZrR_2 + [Ph_3C]^+\left[B(C_6F_5)_4\right]^- \rightarrow [Cp_2ZrR]^+\left[B(C_6F_5)_4\right]^- + Ph_3CR \quad (1.84)$$

(2) Protonolysis

$$\begin{aligned} Cp_2ZrR_2 + [HNR_3]^+\left[B(C_6F_5)_4\right]^- \\ \rightarrow [Cp_2ZrR]^+\left[B(C_6F_5)_4\right]^- + NR_3 + RH \end{aligned} \tag{1.85}$$

$$Cp_2ZrR_2 + \ ROH \cdot B(C_6F_5)_3 \rightarrow [Cp_2ZrR]^+[RO \cdot B(C_6F_5)_3]^- + RH \tag{1.86}$$

(3) Ligand abstraction

$$Cp_2ZrR_2 + B(C_6F_5)_3 \rightarrow \ [Cp_2ZrR]^+\left[RB(C_6F_5)_3\right]^- \tag{1.87}$$

In order to form highly active and stable cationic species, the counter anion should be weakly coordinated to the cationic species and tolerant of the electrophilic attack by the cationic species. Thus, C_6F_5 group is selected and the high activity comparable to the MAO system is achieved by the use of $B(C_6F_5)_3$, $[Ph_3C]^+[B(C_6F_5)_4]^-$ or $[PhNMe_2H]^+[B(C_6F_5)_4]^-$.

1.5.1.3 Structure and Role of MAO

MAO is a condensation product of Me_3Al and H_2O containing linear and cyclic oligomers with various degree of polymerization. Consequently the precise structure and activation process of MAO is not still clear. The structures of cyclic trimer (**1**) and linear tetramer (**2**) are shown in Fig. 1.18.

Sinn et al. proposed the spherical structure **4** composed of four linear tetramers which intramolecularly coordinate to form a cyclic structure, **3** [33]. The nano tube structure **5** with the same chemical composition with **4** is reported to be effective as a cocatalyst by quantum chemical calculation [34].

Barron et al. isolated a compound composed of two molecules of cyclic *tert*-butylaluminoxane trimer **6** and clarified that the distorted Al–O bond activated Cp_2ZrMe_2 as a potential Lewis acid site (Eq. 1.88) [35].

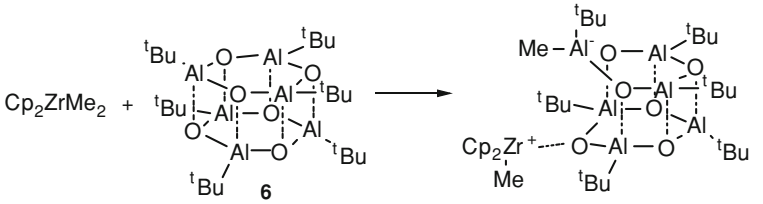

(1.88)

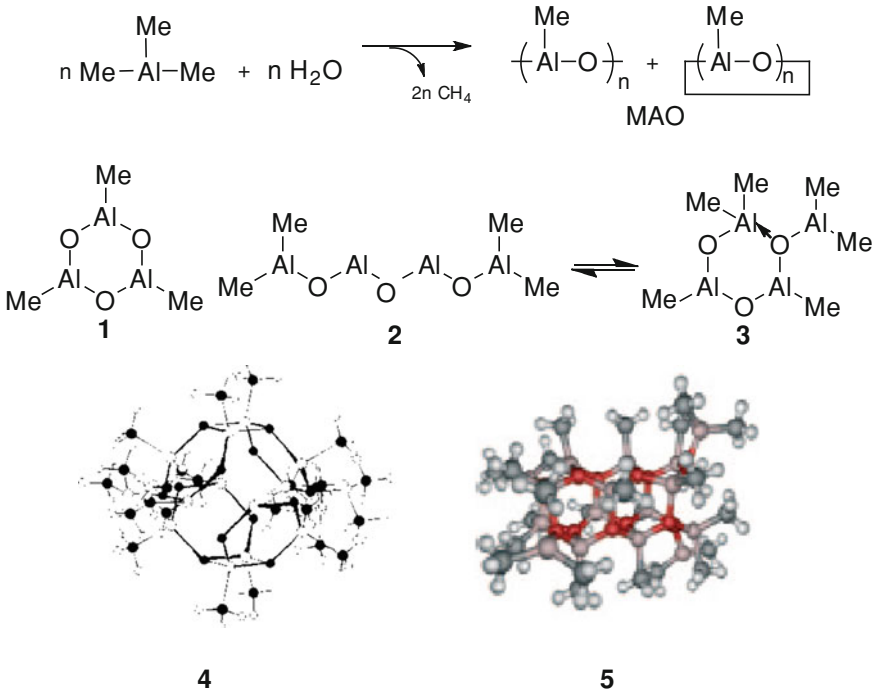

Fig. 1.18 Plausible structures of MAO [33, 34]

MAO contains free Me_3Al and acts as an alkylation reagent and a Lewis acid for the activation of metallocene dichloride (Eq. 1.89).

$$\begin{aligned} Cp_2ZrCl_2 &\xrightarrow[Me_3Al\ in\ MAO]{} \left[\, Cp_2ZrMe_2 \,\right] \\ &\xrightarrow[MAO]{} [Cp_2ZrMe]^+\ Me^-\ MAO \end{aligned} \tag{1.89}$$

When the toluene solution of MAO is dried to remove free Me_3Al, the solubility of MAO is significantly decreased, indicating free Me_3Al donates the solubility of MAO. In order to increase the solubility of MAO, modified MAO (MMAO) is prepared from the mixture of Me_3Al and $^iBu_3Al$. MMAO is commercially available as toluene or hexane solution.

MAO and MMAO are also effective for the activation of various transition metal complexes such as Fe, Ni, Co to cause polymerization or oligomerization of olefins, where they should promote the formation of coordinatively unsaturated cationic metal–alkyl species similarly for group 4 metallocene.

1.5.1.4 Group 3 Metallocene

Trivalent group 3 metallocenes have a tendency to form dimer [36]. Mononuclear trivalent group 3 metallocene possessing hydride or alkyl group, which has the isoelectronic structure of group 4 tetravalent cationic metallocene, conducts polymerization of olefin [37, 38]. Binuclear samarocene hydride, $[(Me_5C_5)_2H]_2$, was dissociated to conduct syndiotactic-specific living polymerization of methyl methacrylate [39, 40]. Divalent samarocene was oxidized via one-electron transfer to monomer to form a binuclear initiator, which was applied for the synthesis of tri-block copolymers [41].

1.5.2 Tacticity Control of Polypropylene

Metallocene catalysts give various kinds of polypropylenes such as highly isotactic, highly syndiotactic, statistically atactic, hemi-isotactic or stereoblock, depending on the structure of bis(cyclopentadienyl) ligand [9]. In this section are explained the relation between the structure of metallocene and the mechanism of stereospecific polymerization.

1.5.2.1 C_{2v}-symmetric Metallocene

In achiral C_{2v}-symmetric metallocene, two coordination sites where monomer and propagation chain occupy are equivalent and the derived coordinatively-unsaturated cationic alkyl species is achiral except the chiral carbon of propagation chain-end. When the effect of the chiral carbon is negligible, atactic polymer is produced (Fig. 1.19).

Ewen investigated the effect of polymerization temperature on propylene polymerization with Cp_2TiPh_2–MAO [42]. The catalytic system gave statistically atactic polypropylene at 25 °C (Fig. 1.20a). The effect of the chain-end chiral carbon was not negligible at lower temperature where the rotation of M–C–C* bonds was suppressed to give isotactic polypropylene by a chain-end controlled mechanism (Fig. 1.20c).

1.5.2.2 *Ansa*-C_2-Symmetric Metallocene

Ansa-C_2-Symmetric metallocene possesses a pair of enantiomers. *rac*-$(CH_2)_2(Ind)_2ZrMe_2$ (**7a**) is shown in Fig. 1.21 as a representative of *ansa*-C_2-symmetric metallocene, where two coordination sites are equivalent and the same prochiral face of propylene is selected after the activation to produce isotactic polypropylene.

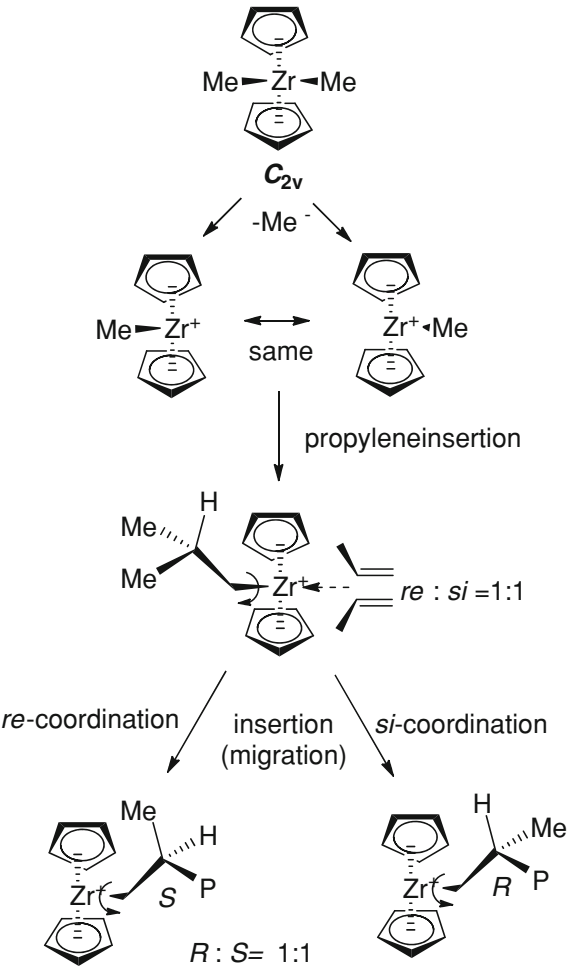

Fig. 1.19 Non-stereospecific polymerization with C_{2v}-symmetric metallocene

Pino et al. clarified how the prochiral face of propylene was selected by *ansa*-C_2-symmetric metallocene [44]. They resolved (−)-*R*-$(CH_2)_2(IndH_4)_2ZrMe_2$ (**8a**) and used it as a catalyst for propylene polymerization in the presence of hydrogen to obtain propylene oligomers. The configuration of the chiral chain-end carbons indicated the coordination state of propylene, where propylene coordinates to the Zr species in order to minimize the repulsion of its methyl group away from β-carbon of the propagation chain which is oriented by the chiral ligand structure (Fig. 1.22). The mechanism is basically the same with that in heterogeneous Ziegler–Natta catalysts proposed by Cossee and Arlman [45, 46] and investigated by Corradini et al. in detail [47].

The results of propylene polymerizations with representative C_2-symmetric metallocenes are summarized in Table 1.1. In *ansa*-bis(indenyl) derivatives, the

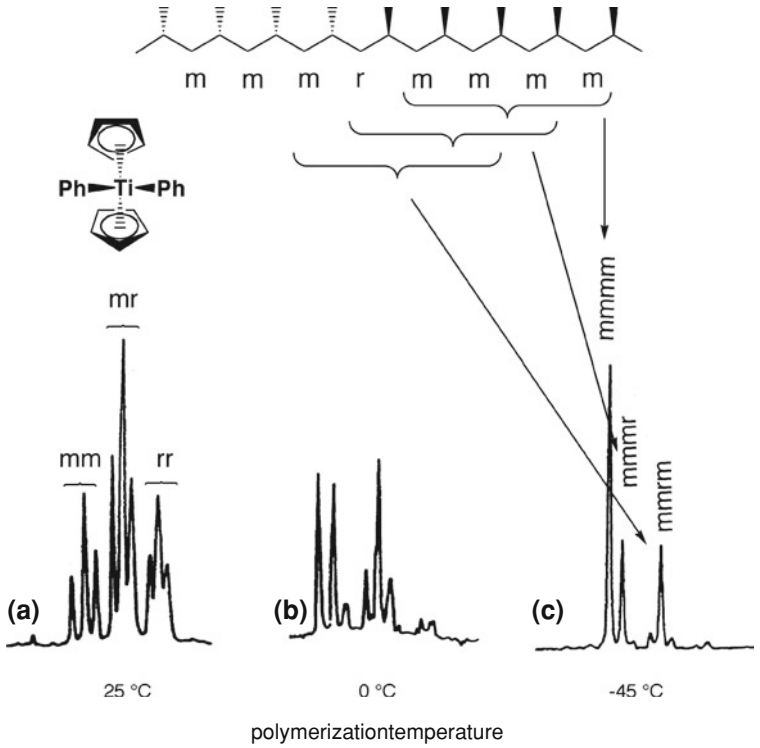

Fig. 1.20 Propylene polymerization with Cp_2TiPh_2–MAO [42]

introduction of bulky substituent at 4-position improved activity and mmmm value. The improvement of isotacticity is explained by the improvement of the selectivity of prochiral face according to the transition state shown in Fig. 1.22. The σ values determined from mmmm are also shown in Table 1.1. The highest σ value reached 0.998 in **14**, which gave the polymer with the melting point of 161 °C. Zirconocene **17** with lower σ values gave the polymers with higher melting points, which is ascribed to high regioselectivity compared with **14**. The rate enhancement should be ascribed to the prohibition of the counter anion coordination by the bulky substituent. The introduction of methyl group at 2-position increased the molecular weight of the polymer produced due to the suppression of chain transfer by monomer (see Sect. 1.5.3)

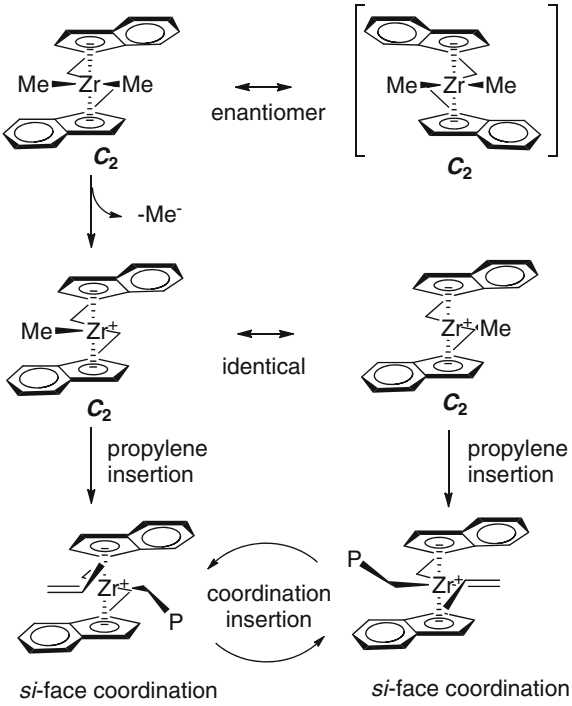

Fig. 1.21 Isotactic-specific polymerization with C_2-symmetric metallocene [43]

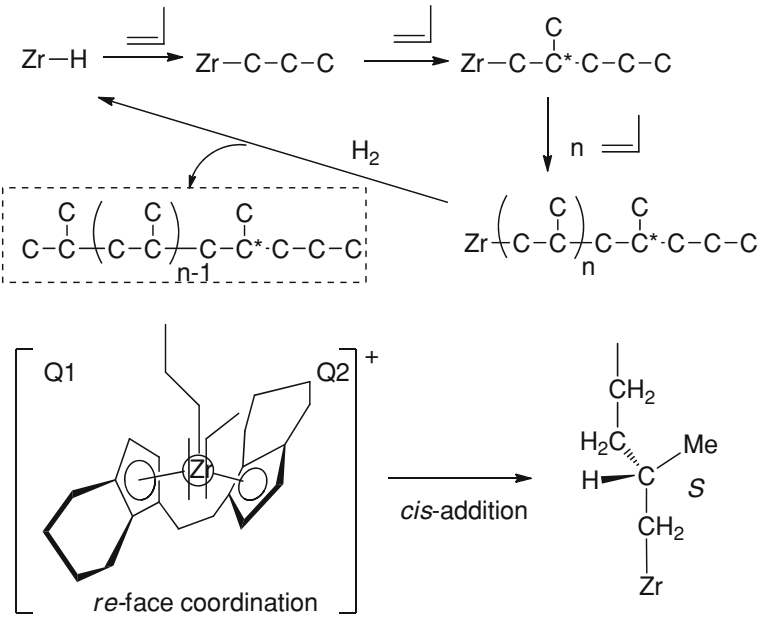

Fig. 1.22 Hydrooligomerization of propylene and its transition state with (−)-*R*-$(CH_2)_2(IndH_4)_2$ $ZrMe_2$–MAO [44]

Table 1.1 Propylene polymerization with C_2-symmetric zirconocene–MAO

Complex[a]	Activity (kg PP/mmol-M/h)	$\bar{M}_w$ ($\times 10^3$)	mmmm[b] (%)	σ[c]	T_m[d] (°C)	Refs.
7b[e]	188	24	78.5	0.952	132	[48]
8b[e]	80	15	–	–	125	[48]
9[e]	190	36	81.7	0.96	137	[49]
10[e]	99	195	88.5	0.976	145	[49]
11[e]	245	213	88.6	0.976	150	[49]
12[e]	403	330	88.7	0.976	146	[49]
13[e]	755	729	95.2	0.99	157	[49]
14[e]	875	920	99.1	0.998	161	[49]
15[f]	16.3	13.7	92.5	0.985	148	[50]
16[f]	11.1	86.5	97.1	0.994	160	[50]
17a[f]	1.59	134	97.7	0.995	162	[50]
17b[f]	0.3	256	98.7	0.997	163	[51]

[a] One of the enantiomers is illustrated
[b] Isotactic pentad
[c] Selectivity of prochiral face of propylene; $\sigma \approx \sqrt[5]{\text{mmmm}}$
[d] Melting temperature
[e] Bulk polymerization, Al/M = 15000, 70 °C
[f] Propylene = 3 kg/cm^2 G, toluene = 500 ml, Al/M = 10000, 30 °C

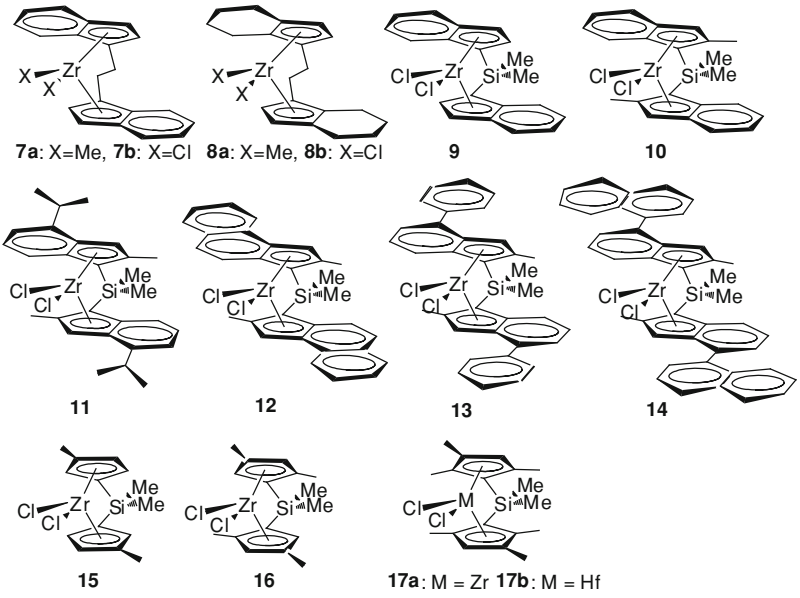

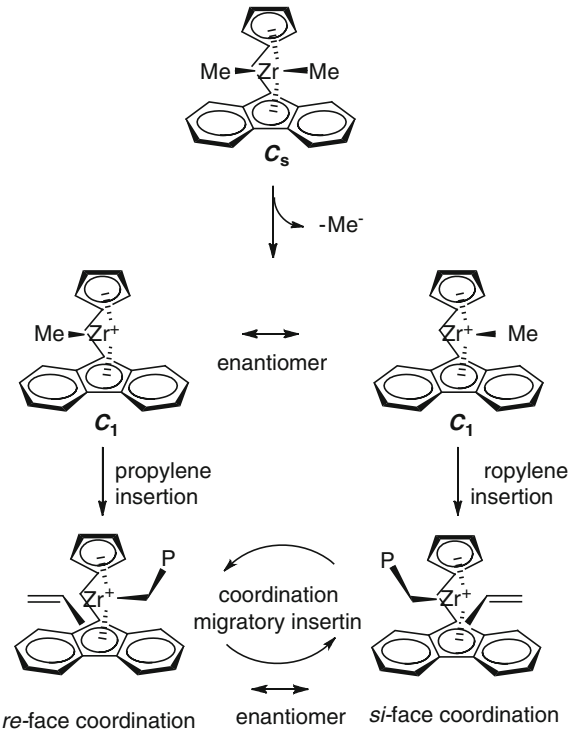

Fig. 1.23 Syndiotactic-specific polymerization with C_s-symmetric metallocene [52]

1.5.2.3 *Ansa*-C_s-Symmetric Metallocene

In *ansa*-C_s-symmetric metallocene, two coordination sites are enantiotopic and the activation of Me^- abstraction gives an enantiomeric pair of active species (Fig. 1.23). Since the propagation proceeds via the migration of the propagation chain, syndiotactic polypropylene is produced by the alternating coordination of *re* and *si* face of propylene on each site. In other words, the production of highly syndiotactic polypropylene with *ansa*-C_s-symmetric metallocene is the experimental evidence that the propagation proceeds via the migration of alkyl chain to the coordinated monomer. The synthesis of highly syndiotactic polypropylene has been realized for the first time by *ansa*-C_s-symmetric metallocene catalyst [52].

If we extend the coordination mode of propylene on the cationic C_2-symmetric metallocene shown in Fig. 1.22, the propagation chain is placed by the repulsion of the ligand and propylene coordinates the Zr species with minimizing the repulsion to the propagation chain.

The results of propylene polymerizations with representative C_s-symmetric metallocenes are summarized in Table 1.2.

Table 1.2 Propylene polymerization with C_s-symmetric zirconocene–MAO

Complex	Temp. (°C)	Activity (kg PP/mmol-Zr/h)	$\bar{M}_w$ ($\times 10^3$)	rrrr[a]	T_m^b (°C)	Refs.
18a	60	435	90	82	137	[52]
18b	60	251	200	88.8	140	[53]
19a	60	152	79	–	134	[54]
19b	60	598	172	–	137	[54]
20a	20	255	1250	93.4	151	[55]
20a	50	721	330	90.6	138	[55]
20b	20	29	980	97.5	151	[55]

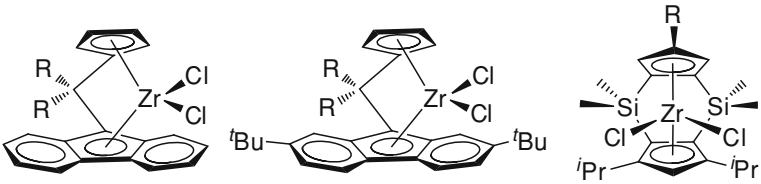

18a: R = Me
18b: R = Ph

19a: R = Me
19b: R = Ph

20a: R = H
20b: R = ^{i}Pr

1.5.2.4 *Ansa*-C_1-Symmetric Metallocene

In *ansa*-C_1-symmetric metallocene, two coordination sites are non-equivalent and the selectivity of the prochiral face of propylene is alternating changed if the propagation proceeds via chain-migratory insertion. When methyl group was introduced at the 3-position of Cp ligand in **18a**, hemiisotactic polypropylene was produced due to the following mechanism. When the propagation chain is located at the methyl-substituted side, the position of the propagation chain cannot be fixed because of the similar steric effect of the methyl and the fluorenyl group to cause no selectivity of the prochiral face of propylene (Fig. 1.24).

When *tert*-butyl group was introduced at the 3-position of Cp ligand in **18b**, isotactic polypropylene was produced. The formation of isotactic polymer is explained by a chain stationary mechanism: the propagation chain cannot be located at the *tert*-butyl-substituted side because of the steric repulsion and always stays at the non-substituted site where the position of the propagation chain can be fixed to select the same prochiral face of propylene (Fig. 1.25).

The relation between the structure of *ansa*-C_1-symmetric zirconocene and the isotactic triad of the obtained polypropylene is shown in Fig. 1.26. Highly isotactic polypropylene was obtained with **24**. *ansa*-C_1-symmetric metallocene such as **21** and **25** has an advantage in the catalyst synthesis compared with C_2-symmetric metallocene and C_1-symmetric metallocene like **22**–**24**: the former gives only an enantiomeric pair, whereas the latter gives a meso form or diastereomers as byproduct.

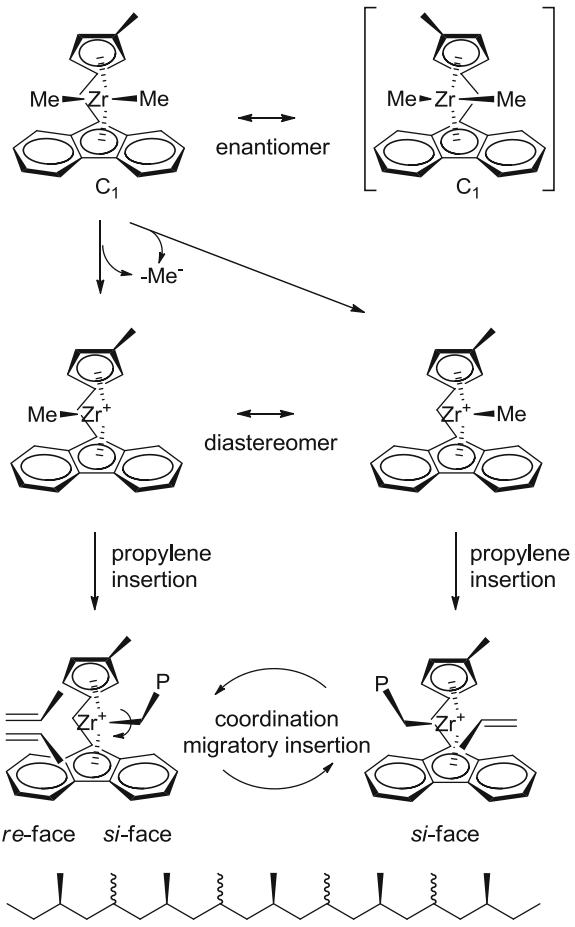

Fig. 1.24 Hemiisotactic-specific polymerization with C_1-symmetric metallocene [56, 57]

1.5.2.5 Stereoblock Polypropylene

Natta obtained stereoblock polypropylene composed of isotactic and atactic segments by the solvent extraction of the polypropylene produced by $TiCl_4$–Et_3Al [61]. The polypropylene showed elastic behavior because of the physical cross-linkage formed by the crystallization of the isotactic segments.

Stereoblock polypropylene was obtained also by *ansa*-C_1-symmetric titanocene [62] and bis(indenyl)zirconocene derivative [63], where the active species reversibly isomerizes between non-stereospecific and isotactic-specific during chain propagation according to the mechanism shown in Fig. 1.27a, b, respectively.

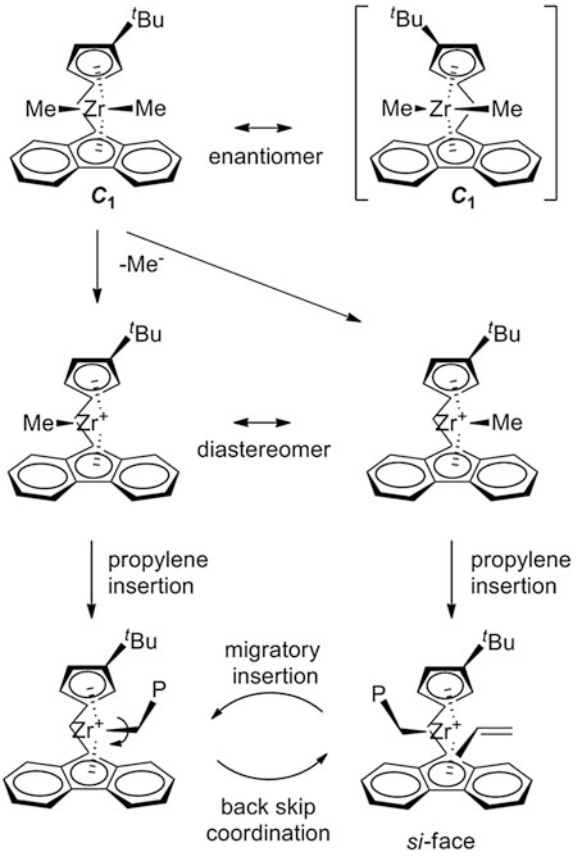

Fig. 1.25 Isotactic-specific polymerization with C_1-symmetric metallocene [56, 57]

1.5.3 Control of Chain Transfer Reaction

In propylene polymerization or copolymerization of ethylene and propylene with Cp_2ZrCl_2-MAO or *rac*-$(CH_2)_2(H_4Ind)_2ZrCl_2$-MAO, β-hydrogen transfer to monomer or to the metal center at the propylene-inserted chain end is predominant to form vinylidene-terminated polymers (Eqs. 1.90 and 1.91).

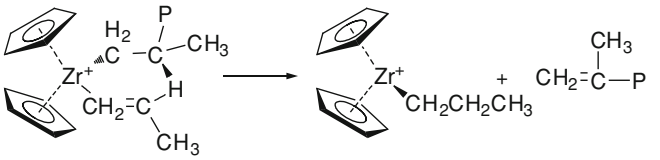

(1.90)

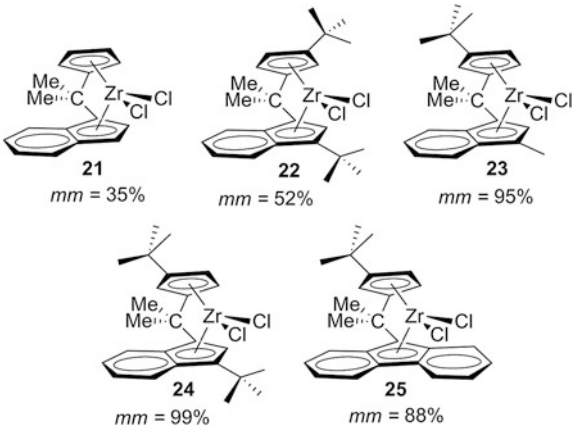

Fig. 1.26 Structure of *ansa*-C_1-symmetric metallocene and isotactic triad of polypropylene obtained [58–60]

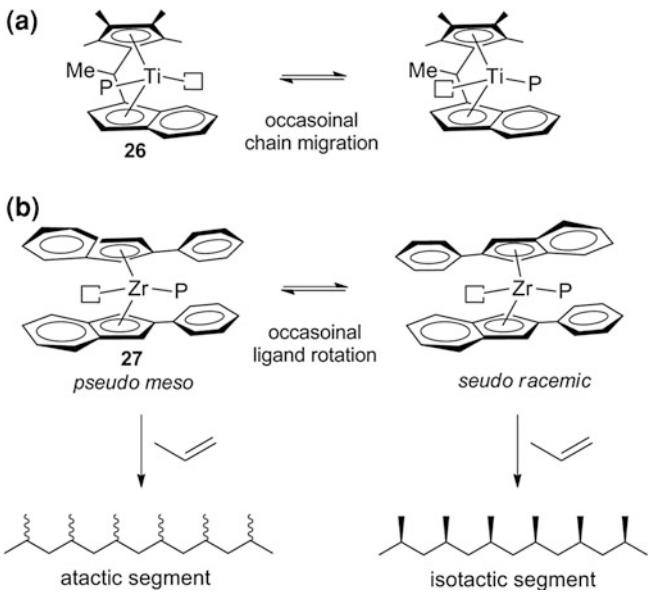

Fig. 1.27 Formation of stereoblock polypropylene by metallocene catalysts: **a** *ansa*-C_1 symmetric titanocene [62], **b** bis(2-phenylindenyl)zirconium derivative [63]

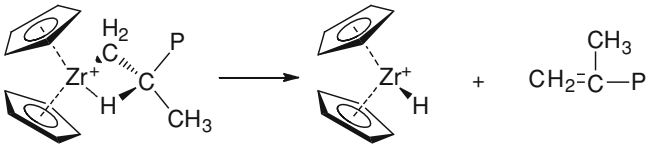

(1.91)

When a hindered metallocene such as $(C_5Me_5)_2ZrCl_2$ is used, β-methyl transfer to the metal center occurs predominantly to give vinyl-terminated polypropylene due to the steric repulsion of the transition state (Eq. 1.92) [64–66].

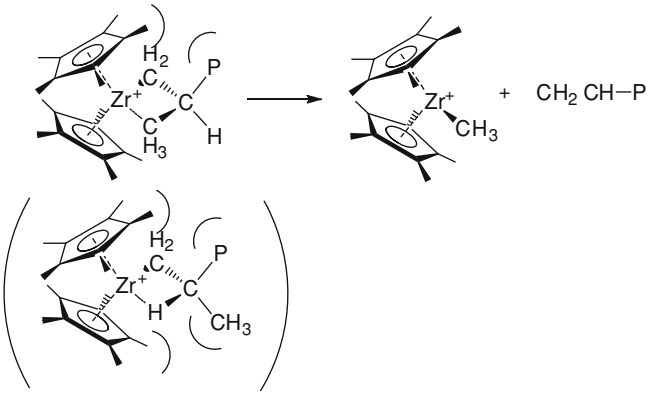

(1.92)

It was considered that chain transfer to coordinated monomer should not be inevitable in olefin polymerization because it is competitive with propagation reaction. However, the introduction of methyl group at 2-position in C_2-symmetric *ansa*-bis(indenyl)zirconocene derivatives was found to suppress chain transfer to monomer to produce high molecular-weight isotactic polypropylene: the steric repulsion of the methyl group prohibits the 6-membered transition state of the chain transfer as shown in Fig. 1.28.

1.5.4 Copolymerization of Olefins

Copolymerization of olefins is very important from the practical point of views. Metallocene catalysts are very important in this field because they copolymerize various olefins in high activity to give uniform copolymers.

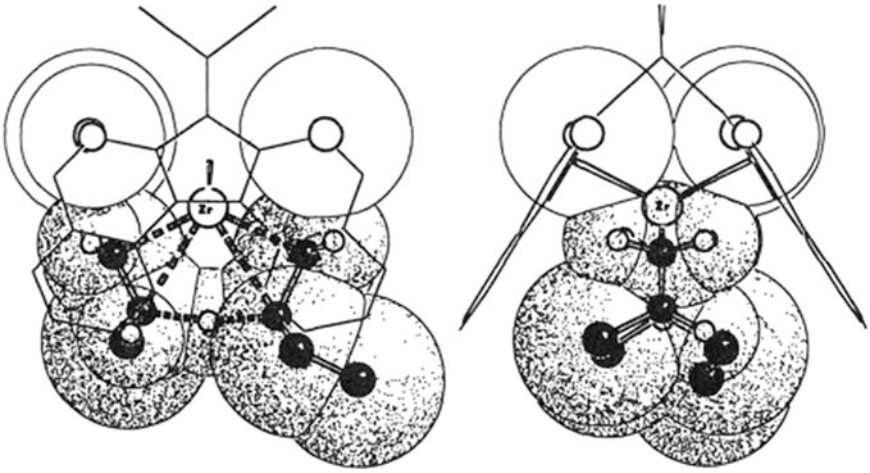

Fig. 1.28 Prohibition of chain transfer to monomer with a sterically-hindered C_2-symmetric metallocene, **11** [49]

1.5.4.1 Copolymerization of Ethylene and 1-Alkene

The majority of LLDPE are produced by highly active $MgCl_2$-supported Ti-based catalysts. However, LLDPE produced by metallocene catalysts has begun to gain share because of its excellent physical properties. Table 1.3 shows the monomer reactivity ratios of ethylene-1-alkene copolymerization with typical metallocene catalysts and those with heterogeneous Ziegler–Natta catalysts for reference.

The $r_E \bullet r_{1\text{-}A}$ values of the metallocene catalysts are approximately one or less regardless of the comonomer employed, indicating random or alternating tendency of these catalytic systems. The r_E values of *ansa*-bis(indenyl) and *ansa*-(cyclopentadienyl)(fluorenyl) derivatives are lower than that of Cp_2ZrCl_2, indicating better copolymerization ability for 1-alkene.

On the other hand, the $r_E \bullet r_{1\text{-}A}$ values of the conventional heterogeneous catalysts are more than one, suggesting the block tendency of the copolymerization. The $r_E \bullet r_{1\text{-}A}$ value of ethylene–1-butene $TiCl_4/MgCl_2$ was reported to be 1.14, suggesting random copolymerization. However, the copolymer obtained was fractionated by diisopropyl ether, hexane and cyclohexane into five parts, and the r_E and $r_{1\ -\ A}$ values of each fraction determined by Eqs. 1.80 and 1.81 were found to vary from 12 to 1 and from 0.1 to 1.1, respectively [72]. The result indicates the presence of multiple active species with different copolymerization ability.

1.5.4.2 Copolymerization of Ethylene and Propylene

EPR and ethylene-propylene-diene terpolymer (EPDM) have been produced by V-based homogeneous Ziegler–Natta catalysts. Metallocene catalysts can be applied

Table 1.3 Monomer reactivity ratios in copolymerization of ethylene and 1-alkene

Catalyst[c]	1-alkene	Temp. (°C)	r_E^a	r_{1-A}^b	$r_E \bullet r_{1-A}$	Refs.
Cp_2ZrCl_2–MAO	1-butene	40	55	0.02	1.10	[67]
Cp_2ZrCl_2–MAO	1-butene	60	65	0.01	0.65	[67]
Cp_2ZrCl_2–MAO	1-butene	80	85	0.01	0.85	[67]
Cp_2ZrCl_2–MAO	1-butene	85	125	0.01	1.25	[67]
Cp_2ZrCl_2–MAO	1-hexene	60	62.3	0.003	0.19	[68]
$(Ind)_2ZrCl_2$–MAO	1-hexene	60	88.0	0.005	0.44	[68]
7b–MAO	1-hexene	60	31.0	0.013	0.40	[68]
8b–MAO	1-hexene	40	12.1	0.028	0.34	[69]
9–MAO	1-octene	40	18.9	0.014	0.26	[70]
10–MAO	1-octene	40	19.5	0.013	0.25	[70]
12–MAO	1-octene	40	10.1	0.118	1.19	[70]
18a–MAO	1-hexene	40	5.7	0.05	0.29	[69]
7b–MAO	4-methyl-1-pentene	40	50	0.004	0.20	[71]
$TiCl_4/MgCl_2$–$AlEt_3$	1-butene	80	3.17	0.36	1.14	[72]
$TiCl_3/MgCl_2$–$AlEt_3$	1-hexene	40	21	0.069	1.45	[73]
Solvay $TiCl_3^c$	1-butene	40	69	0.058	4.00	[74]
Solvay $TiCl_3^c$	1-hexene	40	69	0.033	2.28	[74]
Solvay $TiCl^c$	4-methyl-1-pentene	40	150	0.034	5.10	[74]

[a] Reactivity ratio of ethylene
[b] Reactivity ratio of 1-alkene
[c] Cp_2TiMe_2 was used as a cocatalyst

for the production of these copolymers. Table 1.4 summarizes the monomer reactivity ratios of ethylene–propylene copolymerization with typical metallocene catalysts and those with conventional homogeneous and heterogeneous Ziegler–Natta catalysts.

The $r_E \bullet r_P$ values of V-based homogeneous catalysts are approximately 0.2, indicating alternating tendency of the catalytic systems, although the catalysts need low temperature to form uniform active species. The $r_E \bullet r_P$ values of metallocene catalysts are less than one and scattered depending on the metallocene ligand. In the case of Ti-based heterogeneous catalysts, the monomer reactivity ratios, r_E and r_P, are the average of those of multiple active species, and the $r_E \bullet r_P$ values are approximately two.

Alternating copolymers of ethylene (M_1) and a bulky olefin (M_2) such as isobutene or norbornene are obtained due to the large difference in the polymerization ability between M_1-inserted and M_2-inserted active species. The most typical case is the catalyst that cannot conduct homopolymerization of M_2: poly (M_1-*alt*-M_2) is obtained in the presence of excess M_2. Since olefin polymerization with metallocene catalysts basically proceeds via chain migration to the coordinated monomer, the reactivity of the active species alternating changes in each propagation step if two coordination site of metallocene are non-equivalent such as *ansa*-*meso*-bis(indenyl) or C_1-symmetric metallocenes.

Selecting a suitable metallocene and polymerization conditions, we can synthesize poly(ethylene-*alt*-propylene) as shown in Table 1.5.

Table 1.4 Monomer reactivity ratios in copolymerization of ethylene and propylene

Catalyst[c]	Temp. (°C)	r_E[a]	r_P[b]	$r_E \bullet r_P$	Refs.
Cp_2ZrMe_2–MAO	60	31.5	0.005	0.16	[75]
Cp_2ZrCl_2–MAO	50	16.1	0.033	0.53	[76]
Cp_2ZrCl_2–MAO	40	48	0.015	0.72	[73]
$(Me_5Cp)_2ZrCl_2$–MAO	50	250	0.002	0.50	[76]
Cp_2TiPh_2–MAO	50	19.5	0.015	0.29	[76]
7b–MAO	50	6.61	0.06	0.40	[77]
7b–MAO	25	6.26	0.11	0.69	[77]
8b–MAO	40	11.6	0.084	0.97	[73]
18a–MAO	25	1.3	0.2	0.26	[78]
18a–MAO	40	7.0	0.072	0.50	[73]
VCl_4–$AlEt_3$	30	10.3	0.025	0.26	[79]
$VOCl_3$–Et_2AlCl	30	12.1	0.018	0.22	[79]
$VO(OBu)_3$–Et_2AlCl	30	19.8	0.012	0.24	[79]
TCl_3– $(hexyl)_3Al$	75	15.72	0.110	1.73	[80]
AA $TiCl_3$–Et_2AlCl	70	11.6	0.35	4.06	[81]
Solvay $TiCl_3$–Cp_2TiMe_2	40	10	0.22	2.20	[74]
$TiCl_3$–Et_3Al	40	9.02	0.21	1.89	[73]
$TiCl_4/MgCl_2$/EB–Et_3Al/EB[d]	70	5.5	0.36	1.98	[81]
$TiCl_4/MgCl_2$/2EHA–Et_2AlCl[e]	90	6.0	0.02	0.12	[81]

[a] Reactivity ratio of ethylene
[b] Reactivity ratio of propylene
[c] Metallocenes were activated by MAO
[d] EB, ethyl benzoate
[e] Heptane-soluble system where $MgCl_2$ dissolved in 2-ethylhexan-1-ol (2EHA) was added

Table 1.5 Alternating copolymerization of ethylene and propylene with zirconocene activated by MAO

Zr	E/P[a]	Temp.(°C)	Activity[b]	$\bar{M}_n$ ($\times 10^3$)	$\bar{M}_w/\bar{M}_n$	[EPE] + [PEP] (%)	Refs.
28	1/20	−40	11	3.1	2.1	93	[82]
29	1/9	0	7130	17.6	2	73	[83]
30	1/13	0	–	–	–	77	[83]
31a	1/30	0	20500	12.3	2	84	[84]
31b	1/50	0	20000	293	3.1	89	[84]
32a	1/9	0	480	14.9[b]	–	86	[84]
32b	1/9	0	1540	22.4[b]	–	85	[84]

[a] Molar ratio of ethylene and propylene
[b] kg/mmol-Zr/h

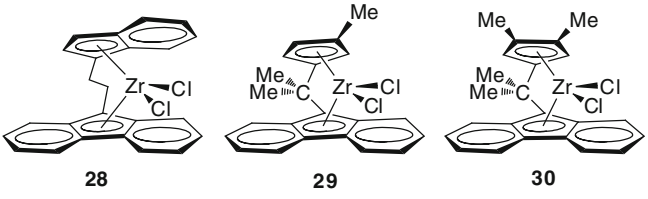

28 **29** **30**

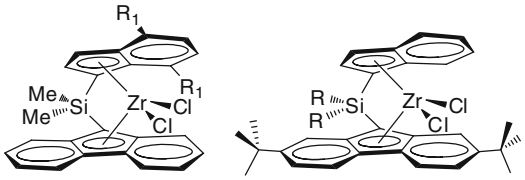

31a: R_1 = H, R_2 = H
31b: R_1 = H, R_2 = Me

32a: R = Me
32b: R = Ph

The mechanisms of the production of poly(ethylene-*alt*-propylene) with C_1-symmetric and C_s-symmetric metallocene are illustrated in Fig. 1.29, where the bulky ligand environment or the bulky chain-end formed by propylene insertion prohibits the coordination of next propylene. The mechanisms correspond to those of stereospecific polymerization of propylene, i.e., catalyst-site control or chain-end control. Figure 1.29a indicates that copolymerization with C_1-symmetric metallocene cannot be analyzed by first-order Malkovian process or a simple terminal model [83, 85].

It is difficult for us to synthesize block copolymers composed of ethylene and propylene by the use of metallocene catalysts because of their poor living polymerization character for both ethylene and propylene. Block copolymers composed of polypropylene and EPR segments were synthesized by $V(acac)_3$–Et_2AlCl, although the polypropylene segment was not crystallized due to the low stereoregularity (rr $\approx$ 65 %) [86]. Development of post-metallocene catalysts have realized living or controlled polymerization of ethylene, propylene and other olefins, which enables us to synthesize various olefin block copolymers possessing the melting points of polyethylene and/or stereoregular polypropylenes [87].

1.5.4.3 Copolymerization of Ethylene and Norbornene

Cycloolefin polymer (COP) and cyclic olefin copolymer (COC), which consist of rigid alicyclic polymer-backbone, are attractive materials because of their good heat and chemical resistance as well as their low dielectric constants, nonhygroscopicity, and high transparency [88]. COP is synthesized via ring-opening metathesis polymerization (ROMP) of norbornene derivatives followed by hydrogenation of C=C bonds in main chain [89, 90], whereas COC via copolymerization of ethylene and cycloolefin such as norbornene.

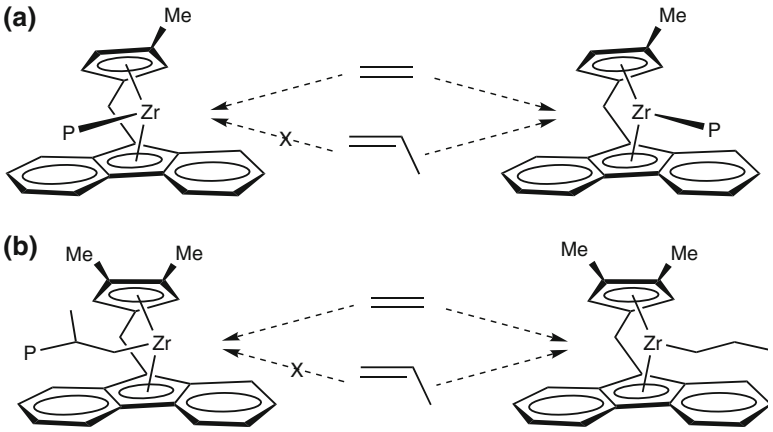

Fig. 1.29 Alternating copolymerization of ethylene and propylene with C_1-symmetric (**a**) and C_s-symmetric (**b**) metallocenes [83]

Table 1.6 Monomer reactivity ratios in copolymerization of ethylene and norbornene[a]

Zr	Symmetry	Temp (°C)	r_E[b]	r_N[b]	$r_E \bullet r_N$	Refs.
Cp_2ZrCl_2	C_{2v}	23	20	<0.1	≈1	[91]
8b	C_2	25	6	0.10	0.7	[91]
9	C_2	30	2.6	<1	≈1	[92]
18a	C_s	30	3.4	0.06	0.2	[92]
18b	C_s	30	3.0	0.05	0.15	[92]
25	C_1	30	3.1	0	0	[92]

[a] Cocatalyst, MAO
[b] r_E and r_N, monomer reactivity ratios of ethylene and norbornene, respectively

Efficient copolymerization of ethylene and norbornene has been achieved by metallocene catalysts. The comonomer sequence of ethylene–norbornene copolymer can be controlled by the metallocene used similarly to ethylene–propylene copolymer described in Sect. 1.5.4.2. Monomer reactivity ratios of typical zirconocenes in copolymerization of ethylene and norbornene are summarized in Table 1.6.

1.6 Conclusion

Development of metallocene catalysts has brought us fruits both in a fundamental and a practical point of view. Metallocene catalysts clarified the mechanism of coordination polymerization of olefins, which had been estimated from the

intensive study on heterogeneous Ziegler–Natta catalysts, owing to the well-characterized active species. Metallocene catalysts have realized the production of uniform copolymers of olefins such as LLDPE, EPR, and COC in high activity. The random copolymerization of ethylene and styrene was also achieved by an *ansa*-zirconocene compound [92].

Of course, metallocene catalyst is not a panacea for coordination polymerization. So-called post-metallocene catalysts as well as half metallocene catalyst have therefore been developed for living polymerization of olefins, stereospecific homo- and copolymerization of styrene and conjugated diolefin, copolymerization of olefin and polar monomer and so on. These topics will be described in the following chapters in detail.

References

1. Ziegler K, Martin H (1956) Makromol Chem 18(19):186–194
2. Natta G, Pino P, Mazzanti G (1955) Chim Ind 37:927–932
3. Galli P, Vecellio G (2001) Prog Polym Sci 26:1287–1336
4. Kashiwa N (2003) J Polym Sci Part A Polym Chem 42:1–8
5. Natta G, Pino P, Mazzanti G, Giannini U, Mantica E, Peraldo M (1957) Chim Ind (Milan, Italy) 39:19–20
6. Breslow DS, Newburg NR (1957) J Am Chem Soc 79:5072–5073
7. Long WP, Breslow DS (1975) Justus Liebigs Ann Chem 463–469
8. Sinn H, Kaminsky W (1980) Adv Organomet Chem 18:99–149
9. Brintzinger HH, Fischer D, Muelhaupt R, Rieger B, Waymouth RM (1995) Angew Chem Int Ed Engl 34:1143–1170
10. Hlatky GG (2000) Chem Rev 100:1347–1376
11. Severn JR, Chadwick JC, Duchateau R, Friederichs N (2005) Chem Rev (Washington, DC, U S) 105:4073–4147
12. Gibson VC, Spitzmesser SK (2003) Chem Rev 103:283–315
13. Huggins ML, Natta G, Desreux V, Mark HF (1966) Pure Appl Chem 12:643–654
14. Soga K, Shiono T, Takemura S, Kaminsky W (1987) Makromol Chem Rapid Commun 8:305–310
15. Grassi A, Zambelli A, Resconi L, Albizzati E, Mazzocchi R (1988) Macromolecules 21:617–622
16. Schuerch C (1959) J Polym Sci 40:533–536
17. Bovey FA, Tiers GVD (1960) J Polym Sci 44:173–182
18. Doi Y, Asakura T (1975) Makromol Chem 176:507–509
19. Kakugo M, Miyatake T, Naito Y, Mizunuma K (1988) Macromolecules 21:314–319
20. Doi Y (1982) Makromol Chem Rapid Commun 3:635–641
21. Mayo FR, Lewis FM (1944) J Am Chem Soc 66:1594–1601
22. Alfrey T Jr, Goldfinger G (1944) J Chem Phys 12:205–209
23. Fineman M, Ross SD (1950) J Polym Sci 5:259–262
24. Pyun CW (1970) J Polym Sci Part A-2 8:1111–1126
25. Harwood HJ, Ritchey WM (1964) J Polym Sci Part A Gen Pap 2:601–607
26. Coleman BD, Fox TG (1963) J Polym Sci Part A Polym Chem 1:3183–3197
27. Takarazaki T (2000) Bunseki (Japanese) 516
28. Andresen A, Cordes HG, Herwig J, Kaminsky W, Merck A, Mottweiler R, Pein J, Sinn H, Vollmer HJ (1976) Angew Chem 88:689–690
29. Jordan RF, Bajgur CS, Willett R, Scott B (1986) J Am Chem Soc 108:7410–7411
30. Gassman PG, Callstrom MR (1987) J Am Chem Soc 109:7875–7876

31. Sishta C, Hathorn RM, Marks TJ (1992) J Am Chem Soc 114:1112–1114
32. Chen EY-X, Marks TJ (2000) Chem Rev 100:1391–1434
33. Bliemeister J, Hagendorf W, Harder A, Heitmann B, Schimmel I, Schmedt E, Schnuchel W, Sinn H, Tikwe L et al (1995) In: Fink G, Muelhaupt R, Brintzinger HH (eds) Ziegler Catalysts, Springer, p 57–82
34. Linnolahti M, Severn JR, Pakkanen TA (2008) Angew Chem Int Ed 47:9279–9283
35. Harlan CJ, Bott SG, Barron AR (1995) J Am Chem Soc 117:6465–6474
36. Yasuda H, Ihara E (1997) Adv Polym Sci 133:53–101
37. Jeske G, Lauke H, Mauermann H, Swepston PN, Schumann H, Marks TJ (1985) J Am Chem Soc 107:8091–8103
38. Jeske G, Schock LE, Swepston PN, Schumann H, Marks T (1985) J ibid 107:8103–8110
39. Yasuda H, Yamamoto H, Yokota K, Miyake S, Nakamura A (1992) J Am Chem Soc 114:4908–4910
40. Ihara E, Morimoto M, Yasuda H (1995) Macromolecules 28:7886–7892
41. Boffa LS, Novak BM (1997) Tetrahedron 53:15367–15396
42. Ewen JA (1984) J Am Chem Soc 106:6355–6364
43. Kaminsky W, Kuelper K, Brintzinger HH, Wild FRWP (1985) Angew Chem 97:507–508
44. Pino P, Cioni P, Wei J (1987) J Am Chem Soc 109:6189–6191
45. Cossee P (1960) Tetrahedron Lett 17–21
46. Arlman EJ, Cossee P (1964) J Catal 3:99–104
47. Corradini P, Barone V, Fusco R, Guerra G (1982) J Catal 77:32–42
48. Wild FRWP, Wasiucionek M, Huttner G, Brintzinger HH (1985) J Organomet Chem 288:63–67
49. Stehling U, Diebold J, Kirsten R, Roell W, Brintzinger HH, Juengling S, Muelhaupt R, Langhauser F (1994) Organometallics 13:964–970
50. Mise T, Miya S, Yamazaki H (1989) Chem Lett 1853–1856
51. Roell W, Brintzinger HH, Rieger B, Zolk R (1990) Angew Chem 102:339–341
52. Ewen JA, Jones RL, Razavi A, Ferrara JD (1988) J Am Chem Soc 110:6255–6256
53. Razavi A, Atwood JL (1993) J Organomet Chem 459:117–123
54. Shiomura T, Kohno M, Inoue N, Asanuma T, Sugimoto R, Iwatani T, Uchida O, Kimura S, Harima S et al (1996) Macromol Symp 101:289–299
55. Veghini D, Henling LM, Burkhardt TJ, Bercaw JE (1999) J Am Chem Soc 121:564–573
56. Ewen JA, Elder MJ, Jones RL, Haspeslagh L, Atwood JL, Bott SG, Robinson K (1991) Makromol Chem, Macromol Symp 48–49:253–295
57. Ewen JA (1995) ibid 89:181–196
58. Ishihara N, Song H, Green MLH (1991) Polym Prepr Jpn 40:265
59. Miyake S, Okumura Y, Inazawa S (1995) Macromolecules 28:3074–3079
60. Razavi A, Atwood JL (1996) J Organomet Chem 520:115–120
61. Natta G (1959) J Polym Sci 34:531–549
62. Mallin DT, Rausch MD, Lin YG, Dong S, Chien JCW (1990) J Am Chem Soc 112:2030–2031
63. Coates GW, Waymouth RM (1995) Science 267:217–219
64. Watson PL, Roe DC (1982) J Am Chem Soc 104:6471–6473
65. Eshuis JJW, Tan YY, Teuben JH, Renkema J (1990) J Mol Catal 62:277–287
66. Mise T, Kageyama A, Miya S, Yamazaki H (1991) Chem Lett 1525–1528
67. Kaminsky W, Schlobohm M (1986) Makromol Chem Macromol Symp 4:103–118
68. Quijada R, Dupont J, Miranda MSL, Scipioni RB, Galland GB (1995) Macromol Chem Phys 196:3991–4000
69. Uozumi T, Soga K (1992) Makromol Chem 193:823–831
70. Schneider MJ, Suhm J, Muelhaupt R, Prosenc M-H, Brintzinger H-H (1997) Macromolecules 30:3164–3168
71. Kaminsky W, Bark A, Spiehl S, Mueller-Lindenhof N, Niedoba S (1988) In: Kaminsky W, Sinn H (eds) Transition metals and organometallics as catalysts for Olefin polymerization, Springer, p 291–301

72. Kuroda N, Nishikitani Y, Matsuura K, Miyoshi M (1987) Makromol Chem 188:1897–1907
73. Soga K, Uozumi T, Park JR (1990) Makromol Chem 191:2853–2864
74. Soga K, Yanagihara H, Lee DH (1989) Makromol Chem 190:37–44
75. Kaminsky W, Miri M (1985) J Polym Sci Polym Chem Ed 23:2151–2164
76. Ewen JA (1986) Stud Surf Sci Catal 25:271–292
77. Droegemueller H, Heiland K, Kaminsky W (1988) In: Kaminsky W, Sinn H (eds) Transition metals and organometallics as catalysts for Olefin polymerization, Springer, p 303–308
78. Zambelli A, Grassi A, Galimberti M, Mazzocchi R, Piemontesi F (1991) Makromol Chem Rapid Commun 12:523–528
79. Cozewith C, Ver SG (1971) Macromolecules 4:482–489
80. Natta G, Mazzanti G, Valvassori A, Sartori G (1958) Chim Ind 40:717–724
81. Kashiwa N, Mizuno A, Minami S (1984) Polym Bull 12:105–109
82. Jin J, Uozumi T, Sano T, Teranishi T, Soga K, Shiono T (1998) Macromol Rapid Commun 19:337–339
83. Leclerc MK, Waymouth RM (1998) Angew Chem Int Ed Engl 37:922–925
84. Heuer B, Kaminsky W (2005) Macromolecules 38:3054–3059
85. Karssenberg FG, Piel C, Hopf A, Mathot VBF, Kaminsky W (2005) Macromol Theory Simul 14:295–299
86. Doi Y, Keii T (1986) Adv Polym Sci 73–74:201–248
87. Edson JB, Domski GJ, Rose JM, Bolig AD, Brookhart M, Coates GW (2009) In: Mueller AHE, Matyjaszewski K (eds) Controlled and Living Polymerizations, Wiley-VCH Verlag GmbH & Co. KGaA, pp 167–239
88. Tritto I, Boggioni L, Ferro DR (2006) Coord Chem Rev 250:212–241
89. Kohara T (1996) Macromol Symp 101:571–579
90. Yamazaki M (2004) J Mol Catal A Chem 213:81–87
91. Kaminsky W, Beulich I, Arndt-Rosenau M (2001) Macromol Symp 173:211–225
92. Kaminsky W (1996) Macromol Chem Phys 197:3907–3945
93. Arai T, Ohtsu T, Suzuki S (1998) Macromol Rapid Commun 19:327–331